




Article

Conservation Assessment of the Stone Blocks in the Northeast Corner of the Karnak Temples in Luxor, Egypt

Abdelrhman Fahmy ^{1,2,3,*} , Eduardo Molina-Piarnas ²  and Salvador Domínguez-Bella ² 

- ¹ Conservation Department, Faculty of Archaeology, Cairo University, Giza 12613, Egypt
² Department of Earth Sciences, Faculty of Sciences, University of Cadiz, Campus Río San Pedro, 11510 Cadiz, Spain; eduardo.molina@uca.es (E.M.-P.); salvador.dominguez@uca.es (S.D.-B.)
³ Rathgen Research Laboratory, National Museums of Berlin, Schloßstraße 1A, 14059 Berlin, Germany
* Correspondence: abdelrhman.fahmy@uca.es or a.fahmy@smb.spk-berlin.de

Abstract: The Karnak Temples complex, a monumental site dating back to approximately 1970 BC, faces significant preservation challenges due to a confluence of mechanical, environmental, and anthropogenic factors impacting its stone blocks. This study provides a comprehensive evaluation of the deterioration affecting the northeast corner of the complex, revealing that the primary forms of damage include split cracking and fracturing. Seismic activities have induced out-of-plane displacements, fractures, and chipping, while flooding has worsened structural instability through uplift and prolonged water exposure. Soil liquefaction and fluctuating groundwater levels have exacerbated the misalignment and embedding of stone blocks. Thermal stress and wind erosion have caused microstructural decay and surface degradation and contaminated water sources have led to salt weathering and chemical alterations. Multi-temporal satellite imagery has revealed the influence of vegetation, particularly invasive plant species, on physical and biochemical damage to the stone. This study utilized in situ assessments to document damage patterns and employed satellite imagery to assess environmental impacts, providing a multi-proxy approach to understanding the current state of the stone blocks. This analysis highlights the urgent need for a multi-faceted conservation strategy. Recommendations include constructing elevated platforms from durable materials to reduce soil and water contact, implementing non-invasive cleaning and consolidation techniques, and developing effective water management and contamination prevention measures. Restoration should focus on repairing severely affected blocks with historically accurate materials and establishing an open museum setting will enhance public engagement. Long-term preservation will benefit from regular monitoring using 3D scanning and a preventive conservation schedule. Future research should explore non-destructive testing and interdisciplinary collaboration to refine conservation strategies and ensure the sustained protection of this invaluable historical heritage.



Citation: Fahmy, A.; Molina-Piarnas, E.; Domínguez-Bella, S. Conservation Assessment of the Stone Blocks in the Northeast Corner of the Karnak Temples in Luxor, Egypt. *Minerals* **2024**, *14*, 890. <https://doi.org/10.3390/min14090890>

Academic Editors: Silvana Fais and Giuseppe Casula

Received: 19 July 2024

Revised: 22 August 2024

Accepted: 27 August 2024

Published: 30 August 2024

Keywords: Karnak Temples; stone blocks; stone decay; stone weathering; quarries; contaminated water; satellite images; conservation

1. Introduction

Stone monuments, which often serve as vital links to our past, face significant threats from a variety of environmental impacts that can accelerate their decay and compromise their archaeological value. Among these, temperature fluctuations, wind erosion, salt attacks, flooding, and earthquakes are particularly detrimental, each contributing to the degradation of these enduring structures in distinct ways. Accordingly, temperature fluctuations can induce thermal stress within stone materials, leading to physical damage, such as cracking and spalling. Repeated cycles of heating and cooling cause expansion and contraction, which can exacerbate existing weaknesses in stone structures [1–4]. For instance, the monuments in Athens and Santorini have experienced deterioration due to the thermal stresses caused by the city's extreme temperature variations [5–7]. Moreover,



Copyright: © 2024 by the authors. Licensee MDPI, Basel, Switzerland. This article is an open access article distributed under the terms and conditions of the Creative Commons Attribution (CC BY) license (<https://creativecommons.org/licenses/by/4.0/>).

wind erosion is another critical factor, particularly in arid and semi-arid regions where abrasive windblown particles can wear away the surface of stone monuments over time. This process not only erodes the stone but can also contribute to the loss of surface detail and inscriptions [8–10]. Wind impact is indeed a critical issue in desert regions, like Egypt and Sudan, where natural forces can significantly affect both the landscape and cultural heritage. In these regions, wind-driven erosion poses serious challenges, particularly for historical monuments and archaeological sites [11]. The Sphinx, Pyramids of Giza, and Dahshur Pyramids, for example, have been subjected to significant wind-driven erosion over millennia [12–14].

Flooding introduces a range of destructive processes, including erosion, sediment deposition, and chemical weathering. The interaction between water and stone can exacerbate the degradation through processes, like hydrolysis and salt migration, as seen in the damage to the historic structures of Venice due to periodic flooding [15,16]. Earthquakes pose a unique threat by causing immediate and often severe structural damage. Seismic activity can lead to fractures, collapses, and displacements within stone monuments, compounding existing vulnerabilities [17–20]. Historical records of earthquakes reveal the extent of damage to sites, such as the columns in the Abakainon necropolis and Temple C of Selinunte in Italy and historical minarets in Egypt, highlighting the long-term impacts of seismic events [21,22]. Water infiltration is also a major contributor to stone decay, particularly in areas where rising groundwater or flooding occurs [23]. The infiltration of water into stone structures can lead to a range of problems, including salt migration, hydrolysis, and biological growth [24,25]. The impact of water infiltration on the ancient city of Alexandria has been well-documented, highlighting the complex interactions between water and stone materials [26–28]. In addition, salt attack, often exacerbated by rising dampness, leads to the crystallization of salts within stone materials, causing expansion and internal damage. This phenomenon, known as salt weathering, can significantly degrade the structural integrity of stone monuments [29,30].

In Luxor and the south of Egypt, many pilot studies were conducted for archaeological construction materials' durability, decay, alterations, analysis, and conservation. Rombolà [31] revealed the archaeological risks and loss detection of the Sphinx Avenue in Luxor using GIS, as well as creating future intervention plans for the conservation and management. Fitzner et al. [32] demonstrated the problems of sandstone as the main building material in upper Egypt. The most dominant forms of weathering are loss of materials, soiling, detachment, and deformations. Moreover, Ahmed [33] studied the urbanization change and agricultural activities' impact on Luxor monuments and informed that, after building the high dam, many changes were observed, such as rising water table, soil salinization, and groundwater contamination, which affect the durability of stone monuments in upper Egypt, specifically Luxor. In the same context, Megahed [34] validated the climate change impact on Horus Temple preservation in Edfu. Agricultural and urban expansion led to urban sprawling and rising subsurface levels, which caused damage and decay to the structural and architectural elements, such as stone bleeding, salt crystallization, deformations, and dissolution. Marey [35] studied the pathologies of the wall paintings in the Temple of Thutmosis III at Karnak. He reported that the sodium chloride and other soluble salts caused alterations in the wall paintings. Fahmy et al. [36,37] analyzed the impact of the Nile River on the building material and stability of Osiris Temple down the hill of Bigeh Island. The results demonstrated that the mineralogical content of two various types of sandstone was affected by the water interaction with clay minerals of sandstone, which affected its durability. In addition, they studied and analyzed the construction materials of the Ramses II/Nero Temple in the El-Ashmounein archaeological site, where salt weathering was the greatest damage factor that affected the building materials and their preservation due to the various sources of contaminated water nearby.

The Temples of Karnak, one of the most significant religious complexes in Egypt, still contain hundreds of scattered stone blocks that necessitate thorough study from both archaeological and conservation perspectives. The preservation and revelation of these

blocks are crucial for future generations. The blocks may contain inscriptions, carvings, or other forms of ancient Egyptian art and writing that provide invaluable insights into the religious practices, historical events, and daily life of ancient Egypt. In addition, these blocks offer clues about the artistic techniques and stylistic changes over time. This paper focuses specifically on the scattered blocks located in the northeast area of Karnak, in front of the Osiris Chapel, examining conditional and conservation standpoints. To achieve a comprehensive understanding, a multi-faceted approach was employed for condition assessment. This involved in situ observation and documentation of decay and alteration patterns, detailed mapping, and the detection of landscape changes over time using temporal satellite images. Additionally, the hydrological context of the area was analyzed to understand its impact on the stone blocks. This multi-proxy approach not only enhances our understanding of the archaeological significance of the scattered blocks but also informs conservation practices aimed at preserving the Karnak Temples for future generations. By integrating various assessment techniques, this study provides a comprehensive evaluation of the scattered blocks, ensuring that both their historical value and physical integrity are maintained.

2. Architectural and Archaeological Context of the Case Study

The Temples of Karnak, located in Luxor (ancient Thebes, in Egypt), represent one of the largest and most significant religious complexes in the ancient world [38]. Primarily dedicated to the Theban triad of Amun, Mut, and Khonsu, this site offers a rich architectural and archaeological context, reflecting over two millennia of continuous building, renovation, and religious practice. Covering over 100 hectares, the Karnak complex is divided into four main precincts: the Precinct of Amun-Ra, the largest and most significant section centered around the Great Temple of Amun; the Precinct of Mut, dedicated to the goddess Mut and located to the south of the Amun-Ra Precinct; the Precinct of Montu, dedicated to the war god Montu and located to the north of the Amun-Ra Precinct; and the Temple of Amenhotep IV (Akhenaten), located to the east and largely dismantled after his reign [39]. Architecturally, Karnak is renowned for its hypostyle hall, particularly the one built during the reigns of Seti I and Ramesses II, which contains 134 massive columns arranged in 16 rows, with the central columns standing 21 m high. The complex also features ten pylons constructed over different periods, serving as monumental gateways, several obelisks erected notably by Hatshepsut and Thutmose III as solar symbols, and a large artificial lake within the Precinct of Amun-Ra used for ritualistic purposes [40]. Archaeologically, the Temples of Karnak underwent various historical developments. Initial construction likely began in the Middle Kingdom (c. 2055–1650 BCE) with modest shrines and structures. During the New Kingdom (c. 1550–1070 BCE), the majority of the current structures were built, reflecting the zenith of Theban power and the prominence of Amun's cult, with significant contributions from pharaohs, such as Thutmose I, Hatshepsut, and Ramesses II. From the Late Period to the Ptolemaic Period (c. 664–30 BCE), the complex saw continued expansions and restorations, including contributions from Nubian pharaohs and Ptolemaic rulers. These phases of construction and renovation highlight Karnak's enduring religious and cultural significance throughout ancient Egyptian history [41].

3. Geographical and Geological Context

The Temples of Karnak are situated in the upper area of Egypt/Luxor city with the coordinates N 25°43'7", E 32°39'31" (Figure 1a,b). The total area of Karnak is around 279.48 km² and the total area of the case study in the northeast corner of the Karnak Temples is around 3.6 km² (Figure 1c). The case study is located around 200 m from the surrounding village of Karnak and around 1 km from the Nile River (Figure 1c). This complex is located on the eastern bank of the Nile River and it is considered an enormous open-air museum and the biggest ancient Egyptian religious community globally.

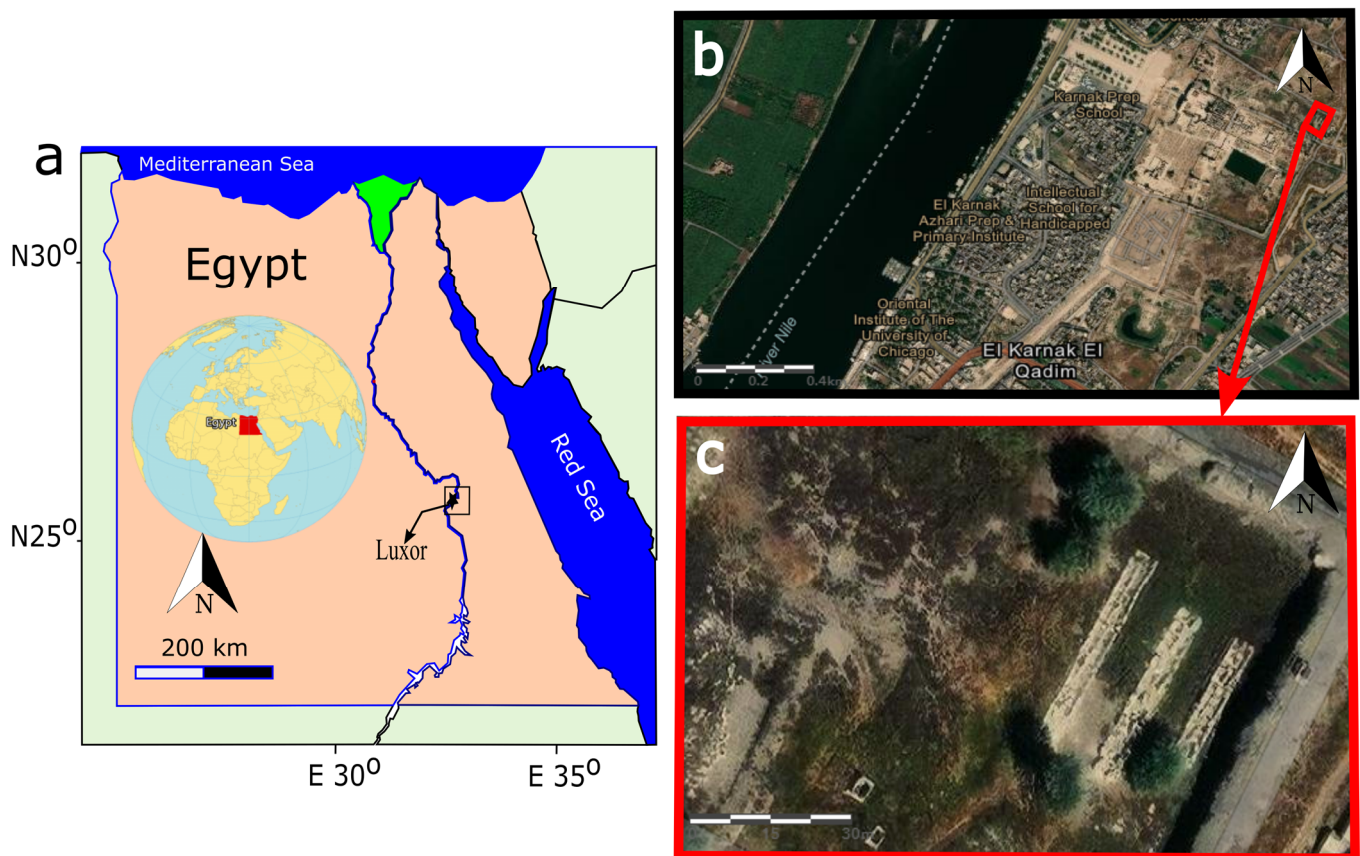


Figure 1. (a) Map of Egypt showing the general location. (b) Hybrid imagery of the Karnak Temple and its surroundings, including rural houses, agricultural lands, and the Nile River. The case study area is marked by a red square in the northeast corner of the Karnak Temples (c).

Geological features of middle and upper Egypt date back to the Eocene age from sedimentary formations (sandstones/siltstone and chalky limestones) with low relief topography (Figure 2) [42]. Luxor geology comprises various units that go back to the Upper Cretaceous, Paleocene–Eocene, Pliocene, and Pleistocene–Holocene [43]. The Pliocene unit is composed of Paleonile river sediments (intraformational conglomerate, red-brown clays with thin fine-grained sand and silt laminae). The Pleistocene unit consists of the Protonile sediments from the Early Pleistocene (pebbly and bouldery gravels), the Prenile sediments of the Middle Pleistocene (fluvial sands with minor gravel and clay beds and loosely consolidated gravel of polygenetic origin), and the Neonile sediments of the Late Pleistocene age (Figure 2). The Holocene unit is formed by the Neonile sediments (silt, micaceous sand, and clays) [43]. The Upper Cretaceous–Early Eocene rock units are unconformably overlain by the Pliocene–Holocene units stratigraphically [44]. The main geological setting of the Karnak Temples is Nile Holocene silty clay along with younger alluvial plains (Figure 2). In addition, the elevation of the Theban plateau is around 300 m above sea level with a sharp scarp encountering the Nile valley on its eastern side (Figure 3) [42]. Around 3.17 km from Karnak in new Luxor city, the soil was characterized by [44]. The mineralogical analysis confirmed that the soil contains smectite minerals as major clay minerals and other clay minerals are present as well, such as kaolinite, chlorite, and illite. In this sense, the presence of such clay minerals can cause a lot of damage to the monuments, bearing soil, foundations, and structural elements because of swelling and shrinkage behaviors.

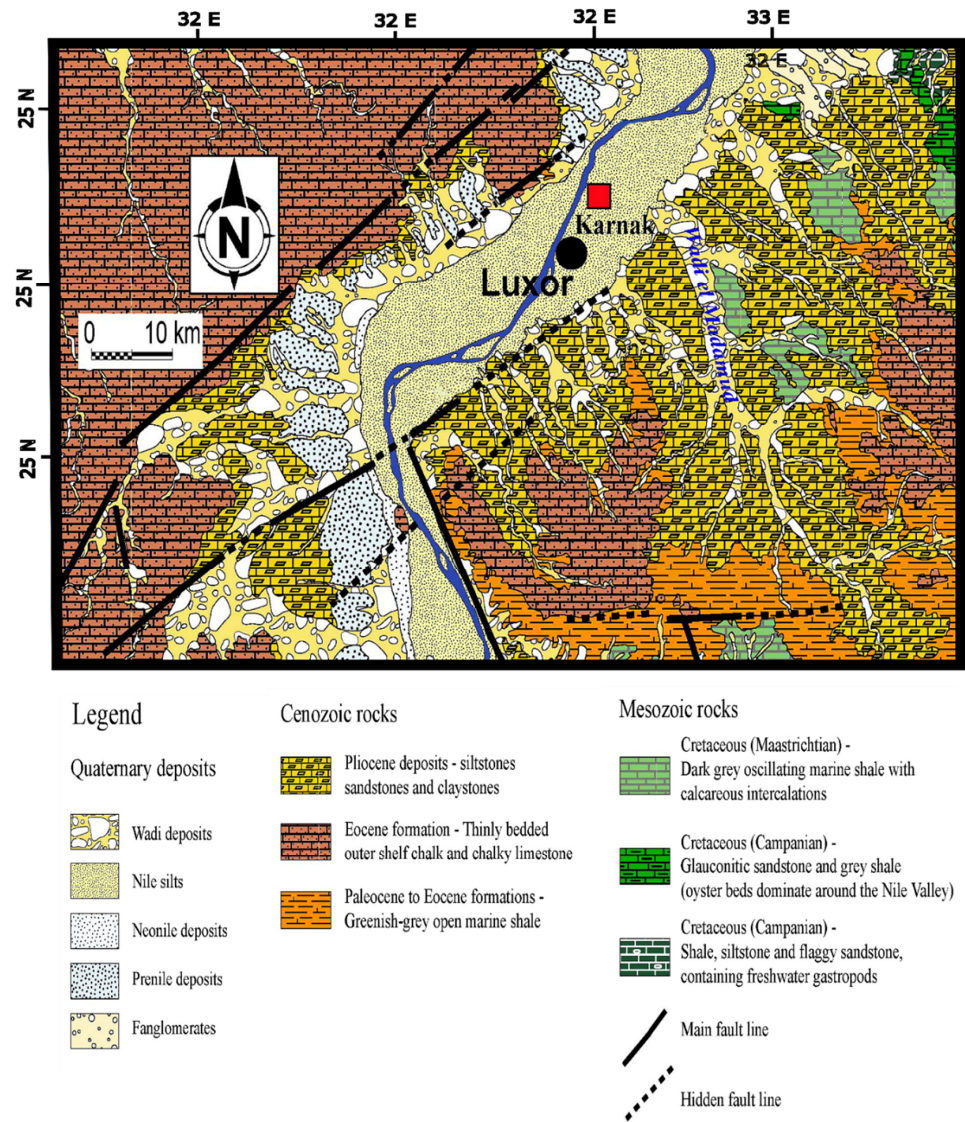


Figure 2. Geological map of Luxor and the Theban Plateau, highlighting the Temples of Karnak and the case study area marked by a red square. Modified after [42].

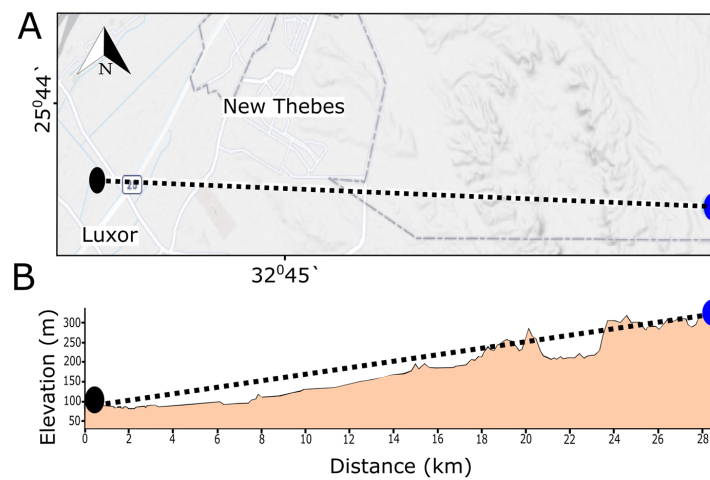


Figure 3. (A) Base map and (B) elevation profile showing the elevation levels of carbonate formations in the Theban area. The black circle marks a point within the Karnak Temples and the blue circle marks a point approximately 28 km to the east.

4. Quarries of Stone Blocks and Mineralogical Characterization

Generally, ancient Egyptians experienced mining and quarrying and they utilized various kinds of stones for structural, architectural, and decorative purposes. Limestone, sandstone, granitoid, basalt, and alabaster/travertine were prepared and cut from several quarries and locations in Egypt [45–47]. These natural stones were used as building and construction materials in the pyramids, temples, and tombs [46]. The main construction material of Karnak monuments is sandstone with high porosity, especially for the stone blocks in the northeast corner. However, red granites, quartzites, limestones, and travertine/Egyptian Alabaster were observed as building materials as well, in a low quantity. Predominantly used sandstone was extracted mainly from Gebel el-Silsila formations (one group of major Nubian Sandstone), which extend from Edfu to Kom Ombo. All sandstone quarries, except the one from Gebel el-Ahmar in Cairo, date back to 65.5–145.5 million years (Cretaceous period) [45]. The ancient name of Gebel el-Silsila is Kheny and this name disappeared in the third intermediate period but in the Roman period was called ‘Sil-sil’/‘Silsilis’ and many outcrops on the east and west banks of the Nile were exploited in the late dynastic to early Roman Period [48–50]. For instance, in the Ramesside era, quarrying activities were very active and intense, especially in the 19th dynasty. Around three outcrops have been confirmed as quarrying areas on the east bank of the Nile River. Moreover, on the west bank (22nd dynasty), quarrying activities were recorded. On the other hand, the east bank (26th dynasty) witnessed quarrying works as well. In the Ptolemaic period, new sandstone blocks were prepared from the west and east banks of sandstone outcrops for temple reconstruction due to interventive restoration works. Furthermore, in the Roman period, various quarries in Gebel el-Silsila were intensively recoured. Around 104 quarries were used in the Roman period and 36 outcrops are assured to have been utilized by Romans on the west and east banks of the Nile River (for example, in Edfu, Dendara, Esna, Medamud, the Temple of Isis, and Min at Koptos) [48]. Two indicators can differentiate between dynastic and Roman quarrying for structural and architectural block preparations. Dynastic blocks are much bigger than Roman ones. Nevertheless, Roman block dimensions are 55–60 cm (in height and depth) and 120–290 cm (in width). In dynastic eras, bronze and copper tools were used for block preparations but Romans were using tools that were made of iron and the tool marks are characterized to be systemic and powerful. Additionally, waste left in the field was much more common in the Roman period than in dynastic eras [48]. Harrel and Storemyr [45] mapped the ancient quarries in the west bank from Naq el-Fugani to Gebel Gulab and they classified the silicified sandstone according to their utilities. For example, there were silicified sandstone for prehistoric tools, grinding stones, and ornamental and building stones. Four samples of sandstone were collected to be classified and studied petrographically by [32]. The first sample (east bank) is a light brown spotted fine-grained sandstone with mainly quartz and secondary constituents, such as rock fragments, clay minerals (kaolinite and clinochlore), opaque matter, feldspar (microcline and albite), muscovite, and heavy minerals with low mechanical strength. The second sample (east bank) is a white spotted fine-grained sandstone with mainly quartz and secondary constituents, such as rock fragments, clay minerals (kaolinite and clinochlore), opaque matter, albite, muscovite, heavy minerals, and small amounts of gypsum and calcite with low to medium mechanical strength. The third sample (west bank) is a yellow-brown very-fine-to-five-grained sandstone with mainly quartz and secondary constituents, such as rock fragments, clay minerals (kaolinite and clinochlore), opaque matter, feldspar (microcline and albite), mica (muscovite, biotite), and heavy minerals with low mechanical strength. The fourth sample (east bank) is a white fine-grained mixture with mainly quartz and secondary constituents, such as rock fragments, clay minerals (kaolinite and clinochlore), opaque matter, and heavy minerals with low mechanical strength [32].

5. Hydrological and Climatological Context

The Temples of Karnak and its stone blocks are surrounded by various water sources, sometimes with contaminated water, that infiltrate the stone and structures through infiltrative phenomena to reach building materials and the sources of water can be the Nile River, canals, drains, aquifers, agricultural activities, and urban waste (Figure 4). A group of researchers collected water samples from the Nile River, nearby canals, agricultural areas, and the sacred lake of the Memnon Temple in the west bank/Luxor to check and analyze the salinity of the water chemically [51]. Results showed the presence of chemical contaminants, such as Sodium (Na^+) (195 ppm in Memnon Temple Lake and 36 ppm in the Nile River), Potassium (K^+) (3.5 ppm in Memnon Temple Lake), Sulfate (SO_4^{-2}) (96 ppm in Memnon Temple Lake), and Chloride (Cl^{-1}) (21 ppm to 190 ppm in Memnon Temple Lake). The possible sources of these chemical constituents are mainly from agricultural irrigation activity and soil dissolution. Subsurface water and high levels of groundwater in the Temples of Karnak were observed between the 1990s and 2006. The water level fluctuations led to the absorption of saline solution triggering the material decay, mechanical decohesion, and subsequent structural instability. In this regard, a groundwater-lowering project and monitoring were conducted from 2007 to 2012, funded by USAID [52]. However, in the summer of 2023, the water rising was observed, also affecting the stone blocks in the Temples of Karnak. Furthermore, the Temples of Karnak are located on two main groundwater aquifers; the shallow Quaternary aquifer (graded sand and gravel with clay with 5 to 95 m thickness and an east to west flow direction) and the Plio-Pleistocene aquifer (sand, clay, and gravel; high salinity) [53]. In this context, groundwater flows from adjacent agricultural areas passing through the Karnak Temples towards the Nile River and the salinity of the groundwater escalates from east to west towards the site and Nile River (Figure 4). Salts trapped within the silty clay led to the increase of salinity under the temples. Additionally, various water samples were collected and analyzed. The results demonstrated that the salinity in the area is very different depending on the site: in the Nile water, it is 173 mg/L; in the canal water, it is 280 m/L; in the drain water, it is 426 mg/L; the water of the sacred lake in Karnak is 780 mg/L; and the groundwater salinity beneath the Karnak Temples ranges from 524 mg/L to 1363 mg/L [53]. The summarized hydrological data context is tabulated in Table 1.

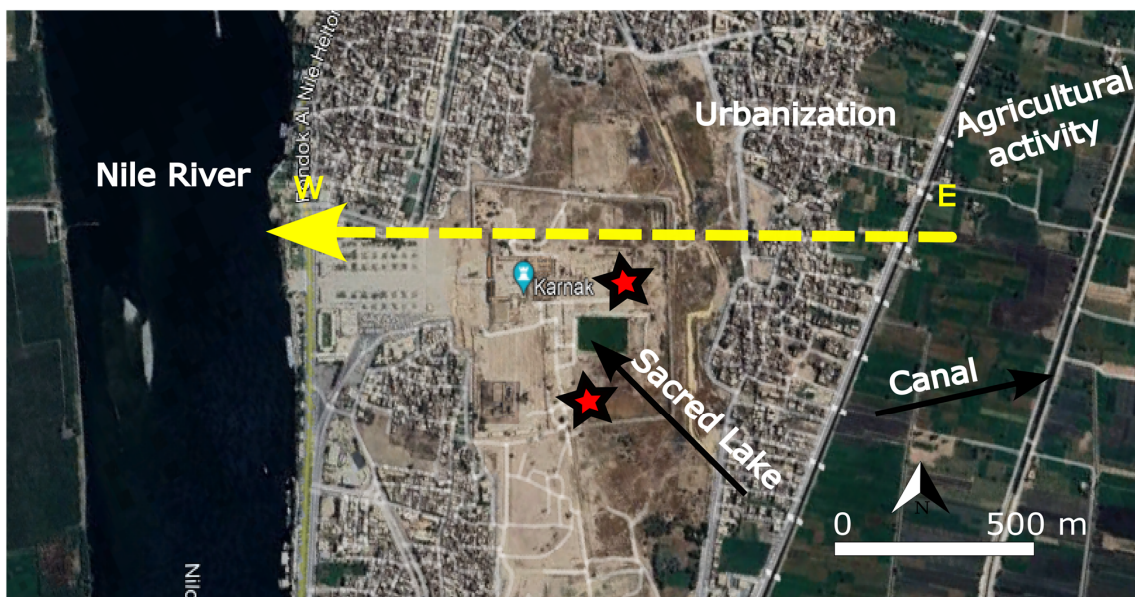


Figure 4. Various contaminated water sources in and around the Temples of Karnak. The yellow arrows indicate the flow direction of water from east to west, originating from canals, drains, cultivated lands, and houses. Salt-contaminated aquifers beneath the Temples of Karnak are marked with stars [53].

Table 1. Summary of hydrological and climatological data for the Karnak area.

Hydrological Context	Details
Main Water Sources	Nile River, canals, agricultural areas, drains, aquifers, urban waste.
Contamination Sources	Agriculture (irrigation), soil and structure dissolution, groundwater salinity.
Water Contaminants	Sodium (Na ⁺), Potassium (K ⁺), Sulfate (SO ₄ ⁻²), Chloride (Cl ⁻¹).
Salinity Levels	- Nile River: 173 mg/L - Canal: 280 mg/L - Drains: 426 mg/L - Sacred Lake: 780 mg/L - Groundwater beneath Karnak: 524–1363 mg/L.
Groundwater Aquifers	- Shallow Quaternary aquifer (5–95 m thickness) - Plio-Pleistocene aquifer (high salinity).
Water Movement and Impact	Groundwater flows from agricultural areas eastward toward the Nile River, increasing salinity levels beneath Karnak.
Rising Groundwater Issue	Periodic water level rise observed since the 1990s. Groundwater-Lowering Project (2007–2012) was conducted but water levels increased again in 2023.
Climate Context	Details
Summer Temperatures	Ranges from 39 to 44 °C (June–September), with very low humidity and almost no rainfall (1–2 mm).
Winter Temperatures	Ranges from 23 to 35 °C (November–April) with cooler nights having temperature drops of 5 °C. Slight rainfall of up to 4.2 mm in May and 0.0 mm in August.
Climate Projections (2100)	Temperature increases of 3–3.5 °C are expected. Rainfall decreases of –5% to 10% are expected.
Wind Conditions	Winds blow from the east. Daily wind speed ranges from 1 m/s to 5 m/s. March 2024 wind speeds: max 7.19 m/s, min 1.02 m/s.

Luxor is dry with low humidity, extremely hot in the summer, and moderately cold in the winter. In the summer (June–September), the temperatures range between 39 and 44 °C. The precipitation is very rare to absent, with around 1–2 mm of rainfall (May–October). On the other hand, in the winter (November–April), the temperatures are between 23 and 35 °C and nighttime is cold, with the temperature being 5 °C lower. Rainfall reaches 4.2 mm in May and 0.0 mm in August [54]. According to future trends and climate change scenarios, the temperature in Luxor will be increased by around 3 to 3.5 by 2100. Additionally, the rainfall will be decreased by –5% to 10% [54]. The wind direction is East and wind speed varies daily from 1 m/s to up to 5 m/s. On 9 March 2024, the maximum speed of wind was 3.08 m/s and the minimum speed was 1.02 m/s. On 10 March 2024, the maximum speed was 7.19 m/s while the minimum speed was 1.02 m/s (<https://meteologix.com/site/selection>; accessed on 1 July 2024). The summarized climatological data context is tabulated in Table 1.

6. Archaeoseismic and Flooding Hazard

Earthquakes and flooding events were considered geohazards that affected the structural stability of the Temples of Karnak. Luxor and its monuments are located around an effective seismic region in south Egypt, especially in Aswan, which experiences many earthquakes, such as being the epicenter in the Aswan area of the 1981 earthquake with 5.6 M, as well as Abu Dabbab (Red Sea) in 1955 with 5.6 M and in 1984 with 5.1 M [55]. Ancient earthquakes of 27 B.C, 600 B.C, and 1200 B.C caused a significant amount of damage to Thebes [56]. In this context, El-Sayed et al. [57] added that Aswan and Kalabsha are considered the most active zones and on March 1969 a very strong earthquake happened with 6.9 M at the entrance of the Gulf of Suez that was felt in and outside Egypt and caused strong damage. Moreover, Karakhanyan et al. [56] carried out a structural analysis for

Colossi of Memnon looking at the evidence of seismic effect and its damage. Structural and ongoing cracking and splitting of the colossus and the pedestals were caused due to seismic events, soil deformation/liquefaction, and subsidence. On the other hand, floods greatly affected the stability of most Egyptian monuments, including the Luxor and Karnak Temples, causing structural deformations and destruction. Before 1960, floods were occurring from June to September [58]. In 1898, B.W Kilburn photographed the first pylon and the forecourt area that was extremely flooded by inundation (Figure 5) [59]. In addition, the Temple of Amenhotep III was flooded with approximately 3 m of the flood basin in the Ramesside period, causing the destruction of the temple. However, earthquakes participated greatly in the destruction of the temple as well [60]. In the same context, Mclane et al. [61] reported that around 24 historical flash floods damaged and caused decay for the Valley of Kings tombs in the west bank/Luxor. In Karnak, the flooding continued and its severity levels changed from 1650 B.C. to the construction of the first Aswan Dam. When Karnak was flooded in a specific area, it returned to its state before construction and that means full destruction. The revealed stela in the third pylon in the Temple of Amon-Re at Karnak led to reports about a great flooding that occurred and inundated the Weskhet-hall of the temple [62].

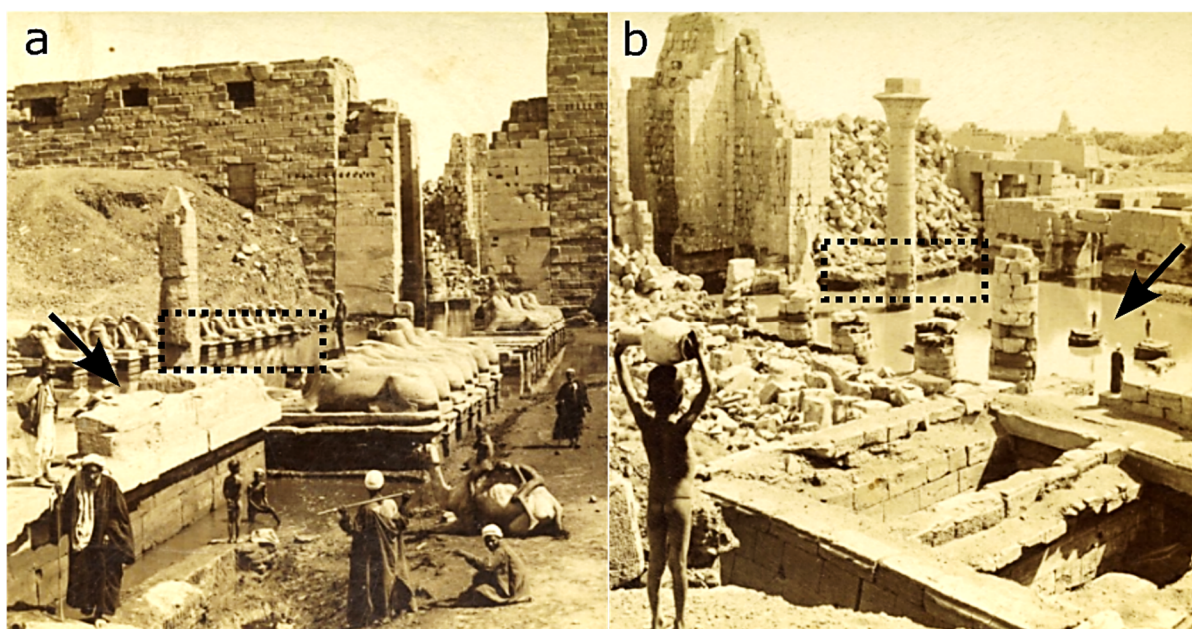


Figure 5. Two historical photographs from 1898 by B.W. Kilburn showing the first pylon of the Karnak Temples. The stone building materials are visibly affected by flash flooding, as indicated by black arrows and highlighted within dotted rectangles (a,b). From [59].

7. Methodology

To thoroughly study and assess the preservation state of the stone blocks in the Karnak Temples, particularly in the northeast corner, an extensive and multi-faceted research methodology was employed. Field trips were conducted to facilitate comprehensive recording, photographing, and measurement of the stone blocks' condition. These field activities were complemented by detailed desk work, which included mapping, engineering, drawing, and site elevation documentation. In addition, satellite imagery and observation played an important role in this study to detect the vegetation change. It was utilized to specify the distribution of the neglected stone blocks across the entirety of the Temples of Karnak, supplementing the insights gained from on-site visits. Furthermore, insights on the quality of ancient quarry stones as sources of Karnak construction materials were discussed.

For land monitoring and biomass change detection in Luxor and the study area within Karnak, the Copernicus collection of 300 m NDVI V2 was employed. This involved synthesizing images over 10-day intervals based on maximum value composition, allowing for precise tracking of vegetation and landscape changes over time. The NDVI V2 time series was derived from the latest reprocessed data from Sentinel-3/OLCAI orbital segments, which provide daily Top of Canopy (TOC) surface reflectance. The 300 m NDVI V2 processing chain included the use of Aerosol Optical Thickness (AOT) data sourced from the Near Real-Time (NRT) database provided by the Copernicus Atmosphere Monitoring Service (CAMS). This comprehensive approach ensured accurate and up-to-date information on vegetation and environmental conditions affecting the stone blocks. This multi-dimensional assessment methodology, combining fieldwork with advanced satellite data analysis, allowed for a thorough evaluation of the preservation state of the stone blocks. By integrating direct observations with remote sensing technologies, this study not only identified the current conditions and distribution of the blocks but also provided valuable insights into the environmental factors influencing their preservation. This integrated approach supports the development of effective conservation strategies to safeguard the stone blocks of the Temples of Karnak for future generations.

8. Results and Discussion

8.1. *In Situ Assessment and Stone Decay*

Field visits and present work were conducted to survey and monitor the locations and condition of all stone blocks in the Temples of Karnak and specify their places and problems. The study area has more than 200 mastabas that carry thousands of dismantled stone blocks. These stone blocks have various dimensions and sizes that range between 100 kg and more than 5 tons. Additionally, these stone blocks were prepared and cut from different materials, such as sandstone (major), limestone, red granite, quartzite, etc. These blocks were parts of the constructed temples, chapels, pylons, and other buildings. Some of these blocks still have aesthetical and epigraphical importance and pigments. From visual observation, conservation, archaeological and management plans, and studies are needed to preserve and reallocate them in harmony with the monuments of Karnak. The positions and places of these forgotten stone blocks were mapped on the master plan of the site (Figure 6). They are distributed and focused in the north, west, and center of the Temples of Karnak. In addition, these blocks were classified into six areas or zones (Figure 6). Google Earth satellite images were prepared to show the actual condition and its situation inside the Karnak complex (Figure 7). In this regard, it is observed that the stone blocks in Areas 1, 2, 3, and 5 are positioned randomly. Figure 6b shows the current landscape of the study area. It consists of three big mastabas and they are marked as m1, m2, and m3, respectively. The m1 contains 59 stone blocks and m2 carries 41 stone blocks while m3 has 43 pieces. Some mastabas were constructed from red brick, filled with sand and rock fragments, and then covered by a cement layer. Additionally, some mastabas were constructed from concrete. The bearing capacity of these mastabas to the stone blocks is insecure and incapable of its functionality. Many fractures, cracks, and deformations were observed. Subsurface water and vegetation damaged, physically and mechanically, these mastabas intended to carry tons of valuable stone blocks. An enormous number of stone blocks were found dismantled and scattered mechanically. In addition, physical and chemical weathering and alterations were observed due to various geoenvironmental and inner defects of natural stone.

Mechanically, seismic and flooding events affected the durability and persistence of the Temples of Karnak throughout the ages. Thousands of scattered and deformed structural and architectural elements were observed due to the accumulative impact of earthquakes and annual flash flooding (June–September) or anthropogenic actions until 1960. Many columns of the temples were dismantled and affected, especially at the bottom of columns that can be damaged because of the high straining action (lateral loads of earthquakes and Nile flooding). The response of using stone blocks as structural materials

to earthquakes was weak, especially with high degrees of ground motion. The stone unities can be separated, deformed, and damaged into scattered pieces with partial and total failure (Figure 8). Earthquakes can cause out-of-plane displacements that lead to severe damage to temple walls due to macroseismic or accumulative microseismical events. Accordingly, roofs, columns, and corners will be affected by various deformations and dismantling (Figure 9(1a,1b)). The damage to building blocks is directly related to primary faulting when the ground transmits the seismic waves from the focus point to the building through the soil and basements [63]. In this sense, Yön et al. [64] demonstrated that out-in plane movements occur during earthquakes. Shear forces and loads for columns, beams, and joints can be increased with seismic events. In addition, columns without a transverse reinforcement in the plastic hinge region manifest low efficacy and capacity towards lateral dynamic loads. Thus, disfiguring and collapse could be observed. In the same context, Kázmér [18] illustrated that chipping, as a damage aspect, can be caused by seismic or /and weathering actions. To differentiate, chippings from seismic events have sharp edges while chippings from weathering are somehow rounded and peeled. Furthermore, unexpected earthquakes occur via connected or /and unconnected fractures through a single or more than two blocks due to the impact of the vertical part of the seismic wave that shakes the blocks up and down rapidly. Additionally, various oriented cracks can be present in a single block or multiple blocks depending on the stone setting. The Temples of Karnak and buildings are settled on silty muddy soil and are considered a weak point and base that accelerate the building collapse and damage.

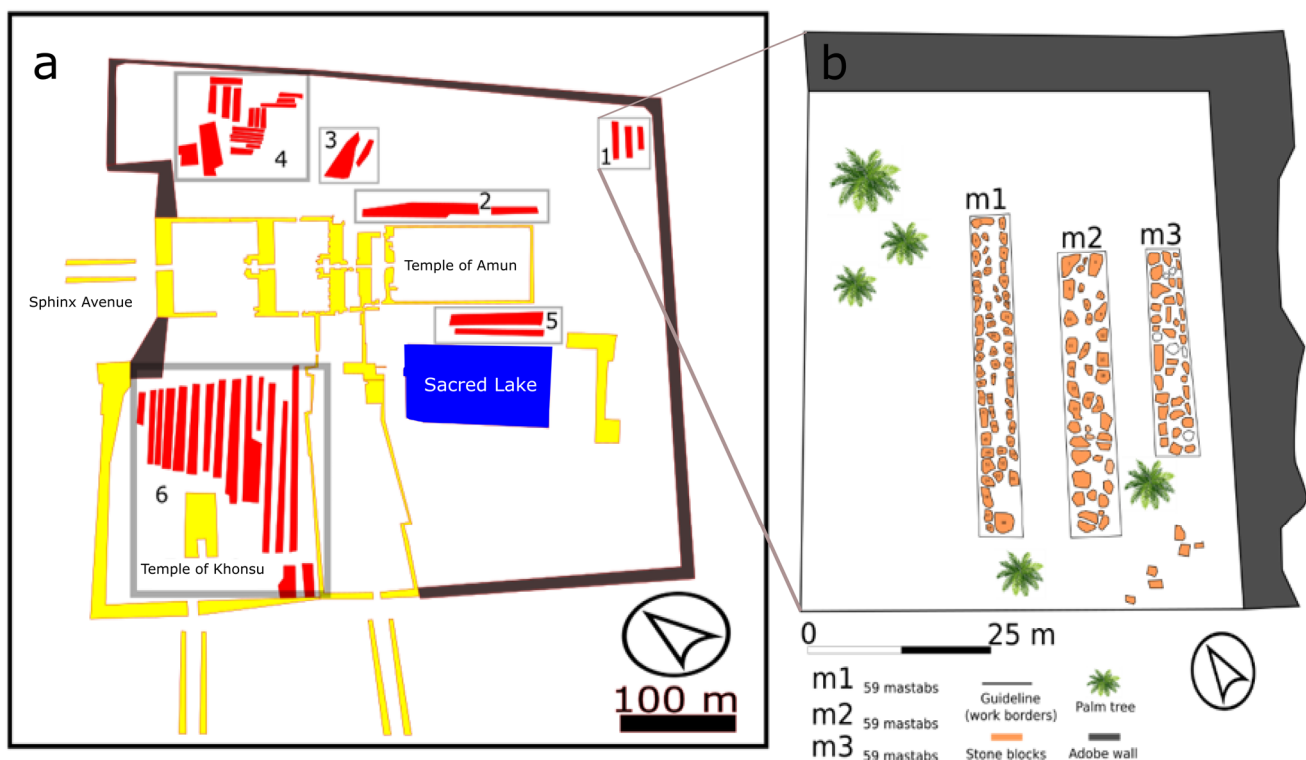


Figure 6. Master plan for the Temples of Karnak. (a) Scattered stone blocks are (in red), divided into six areas. (b) Case study area in the north east corner of the site, with current archaeological landscape.

Additionally, groundwater and water source levels pose significant threats in Karnak. In terms of this concern, soil types, especially clay soils, are very sensitive and mislay their mechanical strength due to the dynamic loads and forces. In the presence of water, soil liquefaction can happen during the earthquake occurrence. This soil liquefaction can cause sliding and collapse of the buildings [65]. The Temples of Karnak and, in the case study, the stone blocks demonstrated damage evidence from earthquakes' impact. For instance,

the decay forms are block fracturing, sharp chippings (dipping broken corners), cracking, and separation (Figure 9(1a,1b,1f,2a,2b)). Fracturing and chipping are the predominant damage aspects in the stone blocks. Stone blocks slipped and embedded into the clay soil are observed as well (Figure 9(1a,1c)).

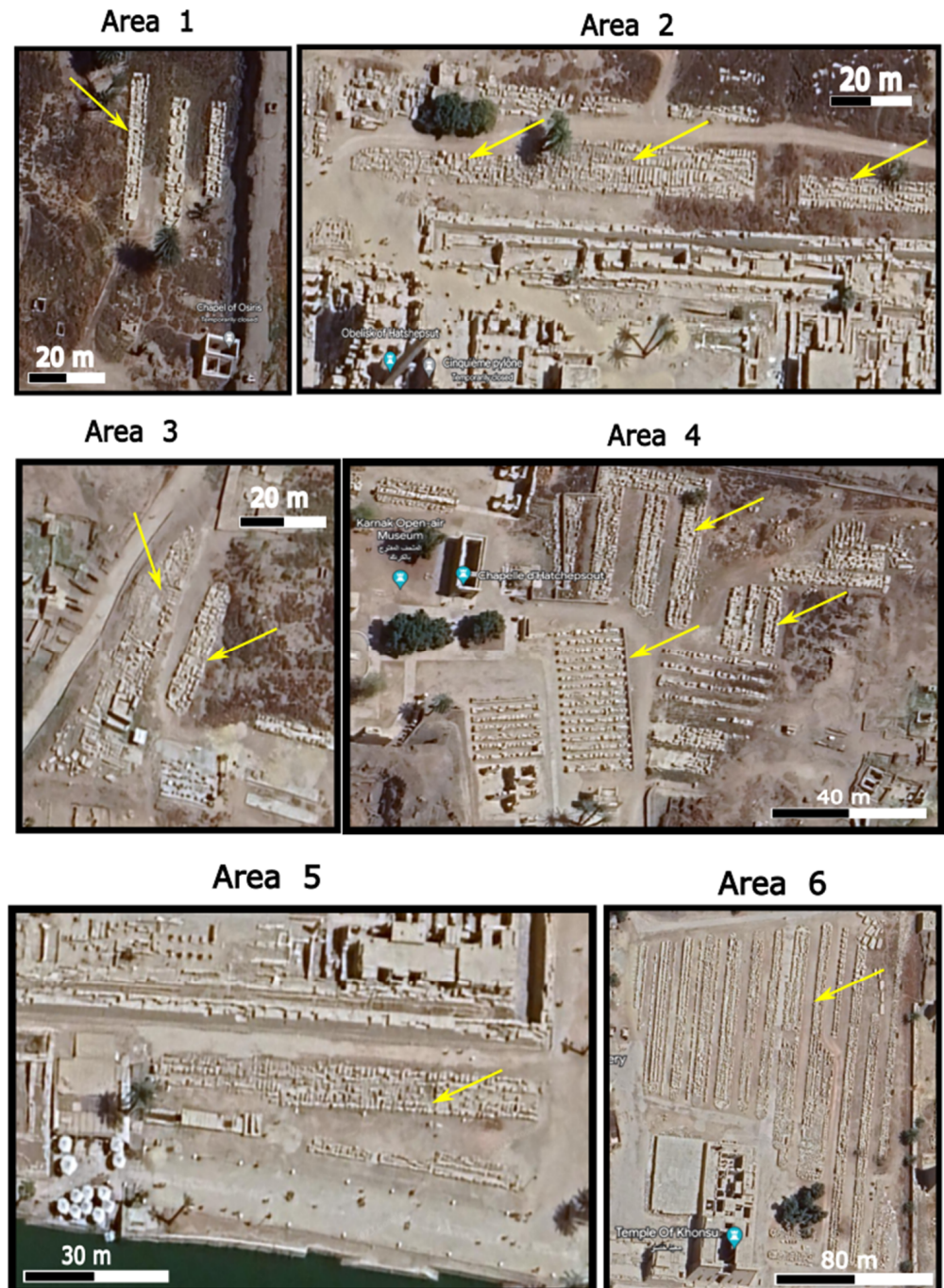


Figure 7. Satellite images depicting six different areas within the Temples of Karnak. The current positions of stone blocks are highlighted by yellow arrows in each image, providing a clear view of their distribution and placement within the temple complex. These images offer insight into the spatial arrangement and condition of the stone blocks, as observed in the present day (Areas 1–6).

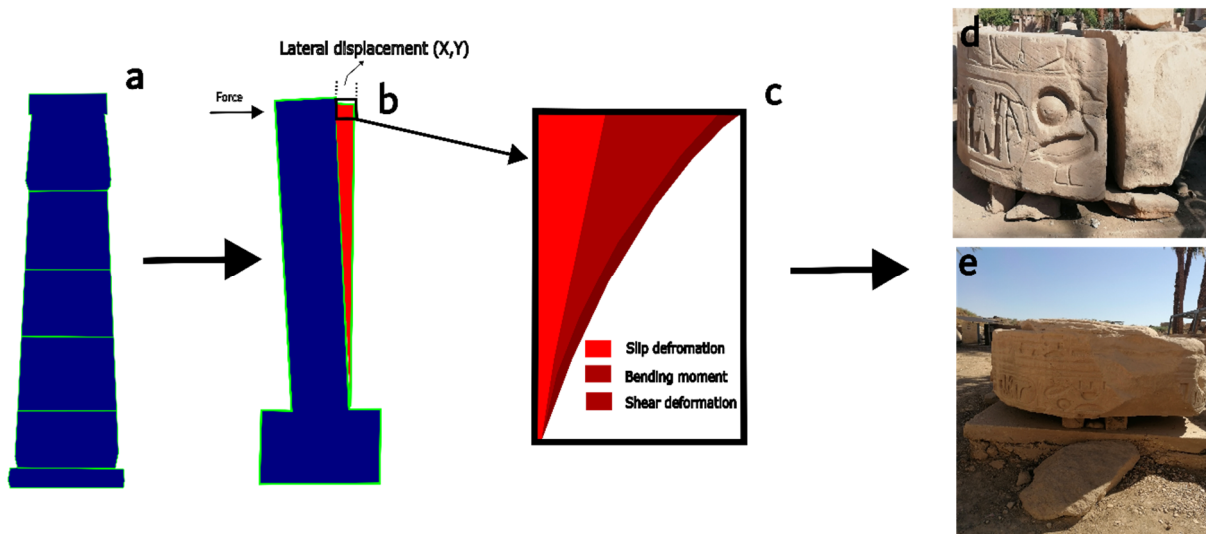


Figure 8. (a–c) Lateral displacements and deformation modes of the stone blocks in the study area in Karnak (d,e).



Figure 9. (1) and (2) Analysis of the mechanical impact of cumulative earthquakes and flooding events on the structures at Karnak. (1a) A general view showing scattered stone blocks, displaced due to mechanical forces, now resting on a loose red brick mastaba. (1b) Close-up of fractured stone blocks, illustrating the damage. (1c) Various stone blocks that have slid and become embedded in the soil, likely as a result of earthquake tremors or the impact of flooding waves. (1d–1f) Detailed views of mechanical chipping, fractures, and cracking observed on the stone surfaces, highlighting the extent of the damage. (2a) A Google Earth image of the study area, focusing on the northeastern part of Karnak, showing the current state of the stone blocks. (2b–2f) Documentation of various damage aspects of the stone blocks, including splitting, chipping, and fracturing, illustrating the ongoing deterioration of the site due to mechanical forces.

On the other hand, the flooding loads are considered a second damage factor of architectural and structural elements in the Temples of Karnak. The flooding ranged between 1 and 3 m in height and caused structural damage to the built temples. Additionally, the presence of water itself caused physical and chemical decay and alterations to stone blocks from the bottom parts of the structures. Accordingly, and hydrostatically, flooding can cause structural failures, uplifting, displacement, deformations, and the overturning of the structures. The flooding damage rate on structures can be affected by stream shape, soil composition, site topography, tree and building positions, and engineering design [66]. Wilk [67] explained the direct damage of flooding waves and surface water, as well as the groundwater flow condition and its increasing level. In this context, this is the same condition for the Temples of Karnak during flooding occurrences. Flooding events, yearly, led to an increase in the water table of the two aquifers and lakes at the site. For this, the damage to the structures and buildings was in Karnak not only from flooding water waves, height, and velocity but also from increasing levels of surface water. Furthermore, fluctuations in the water table can affect the geotechnical problems of the soil, such as changes in soil properties, swelling, shrinkage, and soil settlements [67], and this is what could cause structural damage to the temples and their structures due to the bearing problematic silty clay soil (Figure 9(1c)). Finally, the summarized causes, damage, and decay types are present in Table 2. The table provides a detailed overview of how mechanical forces, such as those from earthquakes and flooding, have impacted the structural integrity of the temple complex.

Table 2. Summary of the types of damage and decay observed in the Temples of Karnak attributed to mechanical loads. This table categorizes various forms of deterioration, including specific damage patterns, such as fractures, chipping, disintegration, and displacement of stone blocks.

Damage Type	Cause	Description	Effects on Structural Elements
Column Dismantling	Earthquakes and Flooding	Columns, especially at the bottom, were damaged due to lateral loads from seismic events and flooding pressures.	Structural instability, potential collapse, and dismantling of columns. Increased shear forces lead to low efficacy under lateral dynamic loads.
Stone Block Fracturing	Earthquakes	Stone blocks were fractured due to seismic waves transmitting through the ground, leading to sharp cracks and breakage.	Out-of-plane movements caused fractures in blocks, separating them into pieces, with partial or total failure. Vertical seismic waves caused rapid up-and-down shaking, worsening the damage.
Sharp Chippings	Earthquakes	Chipping with sharp edges formed during seismic events as a result of the forces applied on stone blocks.	Deformation of the stone surfaces.
Rounded/Peeled Chippings	Weathering	Rounded edges caused by weathering actions.	Gradual degradation of stone elements over time.
Cracking and Separation	Earthquakes and Ground Conditions	Cracking and separation occurred in stone blocks, forming fractures connected or unconnected across one or more blocks.	Stone blocks became separated and dislodged due to vertical seismic movement and unstable soil foundations.
Out-of-Plane Displacement	Earthquakes	The earthquake forces caused sections of walls to shift out of the plane.	Walls sustained severe damage, with deformation, dislodging, and partial collapse.
Soil Liquefaction	Earthquakes and High Groundwater Levels	Soil lost mechanical strength during earthquakes, causing liquefaction.	Structures sank, slid, or collapsed due to weak, liquefied soil.
Embedded Stone Blocks	Earthquakes and Weak Soil	Stone blocks became embedded in the clay soil due to ground subsidence and liquefaction.	Displacement and misalignment of structural blocks within the foundation soil.

Table 2. Cont.

Damage Type	Cause	Description	Effects on Structural Elements
Flooding Uplift and Displacement	Flooding	Hydrostatic forces during floods caused structural uplift and displacement.	Displacement, overturning, or uplift of entire sections of the temple during floods.
Flood-Induced Deformation	Flooding	Water pressure caused deformation, particularly in low-lying parts of structures.	Structural elements at the bottom were physically and chemically altered due to water exposure.
Block Overturning and Sliding	Earthquakes and Flooding	Stone blocks slid or overturned due to dynamic seismic forces or flood water.	Loss of structural integrity as blocks were displaced or completely overturned.
Soil Shrinkage and Swelling	Fluctuating Water Table	Soil changes in response to water level fluctuations caused shrinkage and swelling.	Contributed to the settlement of the structures, weakening the foundations and worsening structural damage over time.
Groundwater Table Fluctuations	Flooding	Increased water table and groundwater flow caused by floods or high surface water levels.	Damage due to changes in soil properties, such as settlement, swelling, and shrinkage. Structural foundations became unstable, leading to long-term deterioration.

8.2. Stone Decay, Alteration, and Water Infiltration

Stone blocks were subjected to various environmental factors, such as temperature fluctuations, wind erosion, rain, etc. In addition, the quality of stone blocks as building materials and their mineralogical content affected their durability as well. Luxor has a clear variation in the temperature from summer to winter. In summer the temperature degrees can reach up to 44 °C and the average temperature is 33 °C. The high temperature in the summer can be a thermal stress/load in the decay and degradation of the sandstone blocks. Accordingly, Shen et al. [68] explained experimentally that sandstone can be subjected to microstructure decay, such as minerals cracking and fracturing during the heating process. Additionally, in the heating period, the quartz mineral particles of sandstone can be changed volumetrically and this can cause microcracks due to the thermal stresses. Many thermal cycles and the accumulative impact of thermal loads can cause disintegration, sugaring, and flaking for the sandstone due to the stress strain actions (Figure 10a–d). Mineralogically, sandstone blocks in Karnak consist of quartz, rock fragments, clay minerals (Kaolinite and clinocllore), opaque matter, feldspar (microcline and albite), mica (muscovite), and heavy minerals. In this sense, the decay and textural features can be changed due to the sandstone composition. For this, Kompaníková et al. [69] demonstrated that sandstone that contains quartz, albite, orthoclase, muscovite, illite, and calcite is much more stable thermally than sandstone that contains chlorite, biotite, dolomite, and kaolinite and concluded that clay minerals and phyllosilicate are the most sensitive in high temperatures and can be structurally disintegrated, affecting the general fabric and color of sandstone. Wind abrasion impact was observed. Many erosion marks on the surface were identified and the erosion led to the distortion of the inscriptions (Figure 10d). Additionally, the wind caused total smoothing to the stone surfaces (Figure 10d). In this regard, after chemical alteration and disintegration due to the cycles of heating and cooling daily, weekly, and annually, wind force can weaken the cementing particles and blow them away [70]. Saltation and deflation are two processes that affect the resistance of the stone block. The main driver of stone saltation is sand and the main driver of stone deflation is the wind shear. During the saltation and deflation processes, the soil around the stone blocks can be removed and migrated to the surface of the stone to form the soiling layer (Figure 10c). Additionally, rain and strong winds can cause significant erosion, leading to the breaking and notching of the blocks. While rainfall typically does not exceed 4.5 mm, it acts as a

catalyst for chemical weathering, reacting with environmental pollutants to accelerate the decay process. Accordingly, ref. [71] confirmed that smoothing, rounding, scouring at the base, pitting, and flaking are the decay patterns on wind and sand loads (Figure 10e,f).

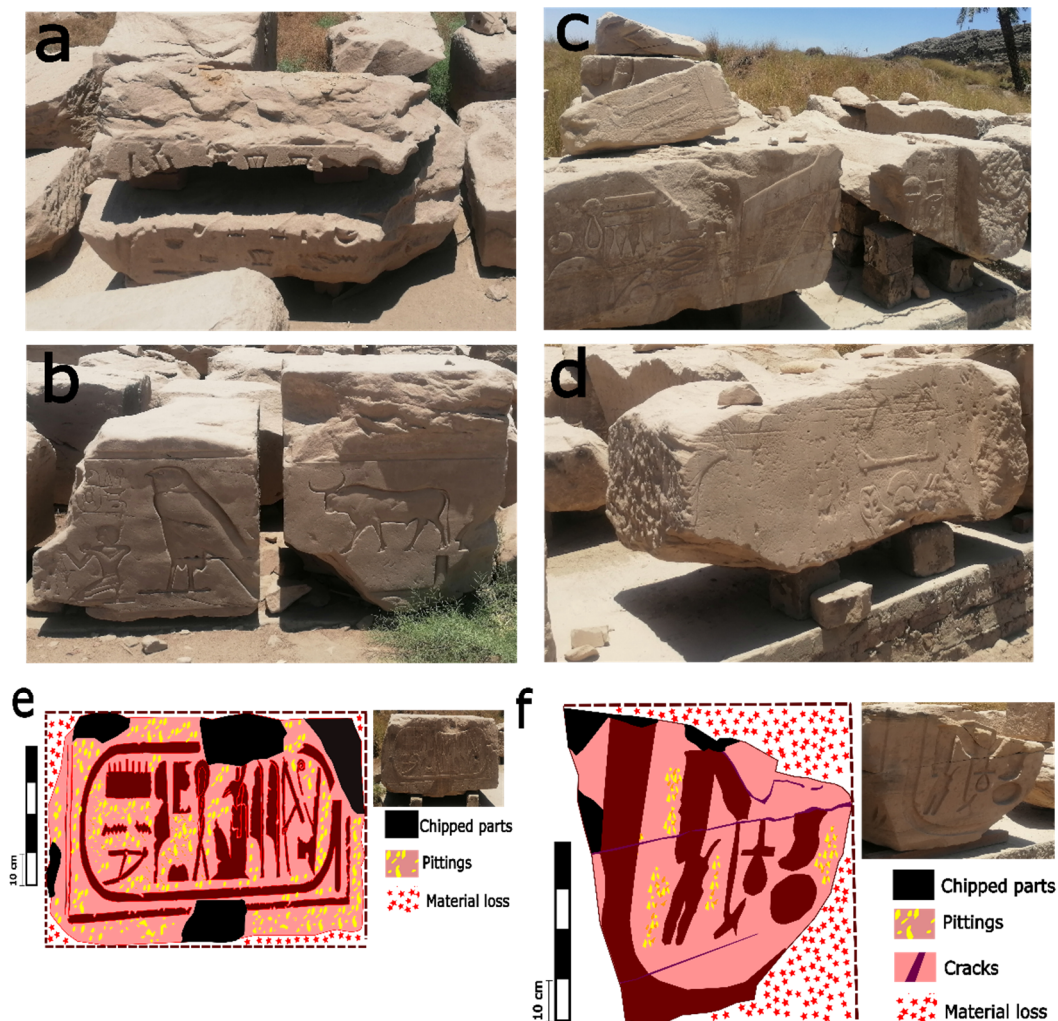


Figure 10. (a–d) Representation of various surface decay patterns observed on stone blocks within the Karnak Temples, including disintegration, flaking, polishing, pitting, and soiling. These patterns illustrate the effects of environmental factors on the stone material. (e,f) Detailed mapping of two specific deteriorated stone blocks, showcasing the extent and types of weathering forms present. This mapping highlights the impact of environmental conditions on the structural integrity of the stone blocks.

Contaminated water infiltration is an important factor in the alteration and degradation. Various sources of contaminated water are affecting the Temples of Karnak, such as water sources from the surrounding urbanization, agricultural activities, aquifers, canals, sacred lakes, the Nile River, and rain. Water sources were elevated and linked to the Temples of Karnak. The elevations were carried out from the east towards the Nile River and from the west towards the urban/rural and cultivated area around the archaeological site (Figure 11a–c). Contaminated components from various sources around the Temples of Karnak area were proven and studied [51,53]. Salts, such as sodium chloride (NaCl) and potassium sulfate (K_2SO_4), are the most common contaminants that were detected causing the salt weathering to the stone blocks. The salt ions can immigrate through the soil to the blocks, leaving the salts on the surface (subefflorescence) or beneath the stone surface (efflorescence) [46,72]. In the same context, salt weathering and attack

on stone blocks are subjected to sequential steps: (1) transportation, (2) accumulation, (3) solute concentration, (4) precipitation, (5) fractionation, (6) local concentration, (7) local salt creeping in case of the capillarity [73]. NaCl-soluble salt crystals grow up in the largest pores and then in the smaller pores and the pressure of the crystal growth in the small pores is much more powerful [74]. Consequently, a lack of mechanical strength, breaking, and disintegration can be observed on stone surfaces (Figure 11d,e). On the other hand, clay minerals inside the sandstone of the blocks can be a serious inner defect with water presence. The chemical and petrographic analysis by [32] for four samples from various siliceous sandstone quarries as stone block sources confirmed presence of clinocllore ($(\text{Mg}, \text{Fe}^{2+}, \text{Al})_3[(\text{OH})_2 | \text{AlSi}_3\text{O}_{10}] \cdot (\text{Mg}, \text{Fe}^{2+}, \text{Al})_3(\text{OH})_6$) and kaolinite ($\text{Al}_2\text{Si}_2\text{O}_5(\text{OH})_4$) as clay minerals. Accordingly, clinocllore is a phyllosilicate mineral (trioctahedral) and one of its characteristics is the exfoliation phenomena, mechanically [75]. However, chlorites are considered non-swelling clays; it is believed that mixed clay minerals can be considered swelling clay [76]. Clinocllore and kaolinite could be a swelling mixed clay and affected the durability of the blocks, causing flaking and exfoliation decay patterns in the presence of water (Figure 11c,e). Finally, Table 3 displays the summarized various decay and damage patterns regarding environmental and stone quality factors.

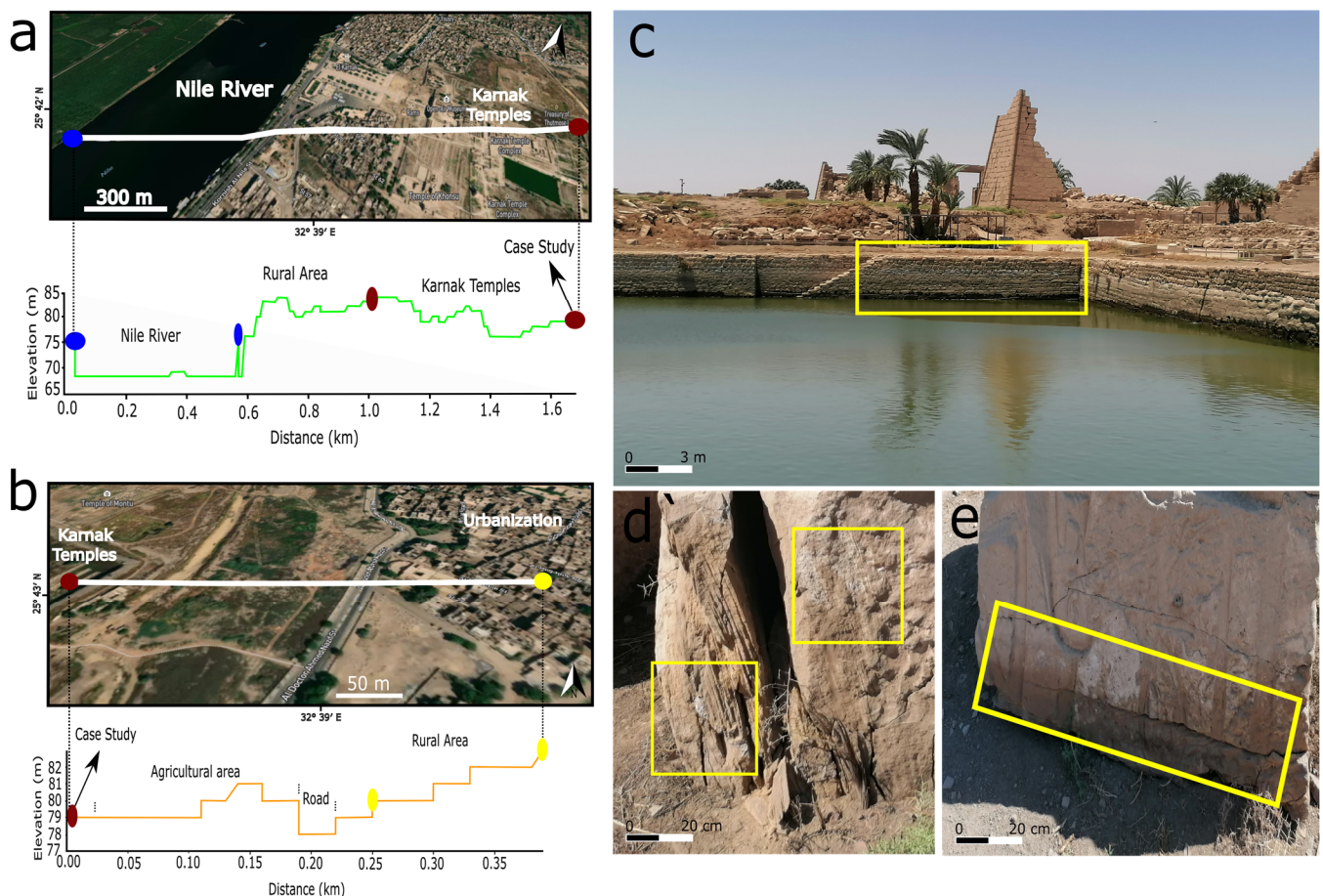


Figure 11. (a) Location of the case study area within Karnak, showing its elevation and relative position with respect to contaminated sources from east to west, based on global digital elevation models. (b) Elevation profile from west to east. (c) Sacred lake within the Temples of Karnak, with a yellow rectangle indicating the fluctuating water levels, which have led to the deposition of precipitates and soiling on the stone surfaces. (d,e) Examples of block surface disintegration and salt damage resulting from water impact.

Table 3. Different types of damage and decay affecting sandstone blocks in Karnak, based on the environmental factors and mineralogical content.

Type of Damage/Decay	Cause	Description/Effect
Thermal (Stress/Load)	Temperature fluctuations	Microstructure decay (mineral cracking and fracturing), volumetric changes in quartz leading to microcracks, sugaring, flaking, and disintegration.
Mineralogical Decay	Composition of sandstone (quartz, albite, muscovite, etc.)	Sandstone with chlorite, biotite, dolomite, and kaolinite is less thermally stable. Clay minerals (e.g., kaolinite, illite) and phyllosilicates disintegrate at high temperatures.
Wind (Erosion/Abrasion)	Wind-driven sand and particles	Surface erosion, distortion of inscriptions, total polishing, rounding, scouring, pitting, flaking, and weakening of cementing particles.
Salt Weathering	Salts from contaminated water sources	Salt ions (NaCl, K ₂ SO ₄) migrate through the soil and block the surface, leading to subefflorescence and efflorescence. Crystal growth in pores causes internal stresses and disintegration.
Capillary Action (Salt Creep)	Water movement through pores	Damage is caused through transportation, accumulation, solute concentration, precipitation, crystal fractionation, and the creeping of salts causing internal and surface damage.
Contaminated Water Infiltration	Water sources (urbanization, agriculture, canals, Nile, rain)	Waterborne contaminants lead to salt deposition, mechanical weakening, and breakage of the stone blocks.
Clay Swelling and Exfoliation	Presence of swelling clays (clinochlore, kaolinite)	Swelling of clay minerals in sandstone leads to inner defects, causing flaking and exfoliation, especially in the presence of water.

8.3. Vegetation Change Detection

Copernicus Global (NDVI raster 300 V2) was used for the observation and detection of the vegetation change using mid to low spatial resolution. NDVI is an indicator to quantify the vegetation's greenness and density. Measurement of NDVI can be calculated through Formula (1):

$$\text{NDVI} = (\text{REF}_{\text{nir}} - \text{REF}_{\text{red}}) / (\text{REF}_{\text{nir}} + \text{REF}_{\text{red}}) \quad (1)$$

where REF_nir and REF_red are the spectral reflectances measured in the near infrared and red wavelengths, respectively.

Figure 12a,b and Table 4 show the multi-temporal analysis and monitoring of the vegetation index and biomass in the Luxor city and case study area (in and around Karnak) from August 2023 to February 2024. For vegetation coverage and density, NDVI values range from −1.0 to 1.0. Negative values indicate water presence and positive values near zero refer to bare soil. In addition, values from 0.1 to 0.5 refer to sparse vegetation and values from 0.6 and up are referring to dense green vegetation. Accordingly, the results (Figure 12b) illustrated the observed variation of vegetation coverage temporally from bare to dense vegetation, which confirms the activity of water resources and its fluctuations in the Karnak area. For instance, in August and September 2023, the vegetation coverage fluctuation was slightly observed. The values were slightly increasing in the last ten days of August and September and some parts were densely covered with vegetation. In January and February, variations of vegetation mass were observed, especially between the last ten days in January (sparse) and the first ten days (dense). Figure 12c,d shows the vegetation and plants around the stone blocks, as well as the biophysical and biochemical impact of the vegetation and plants on the stone blocks' resilience.

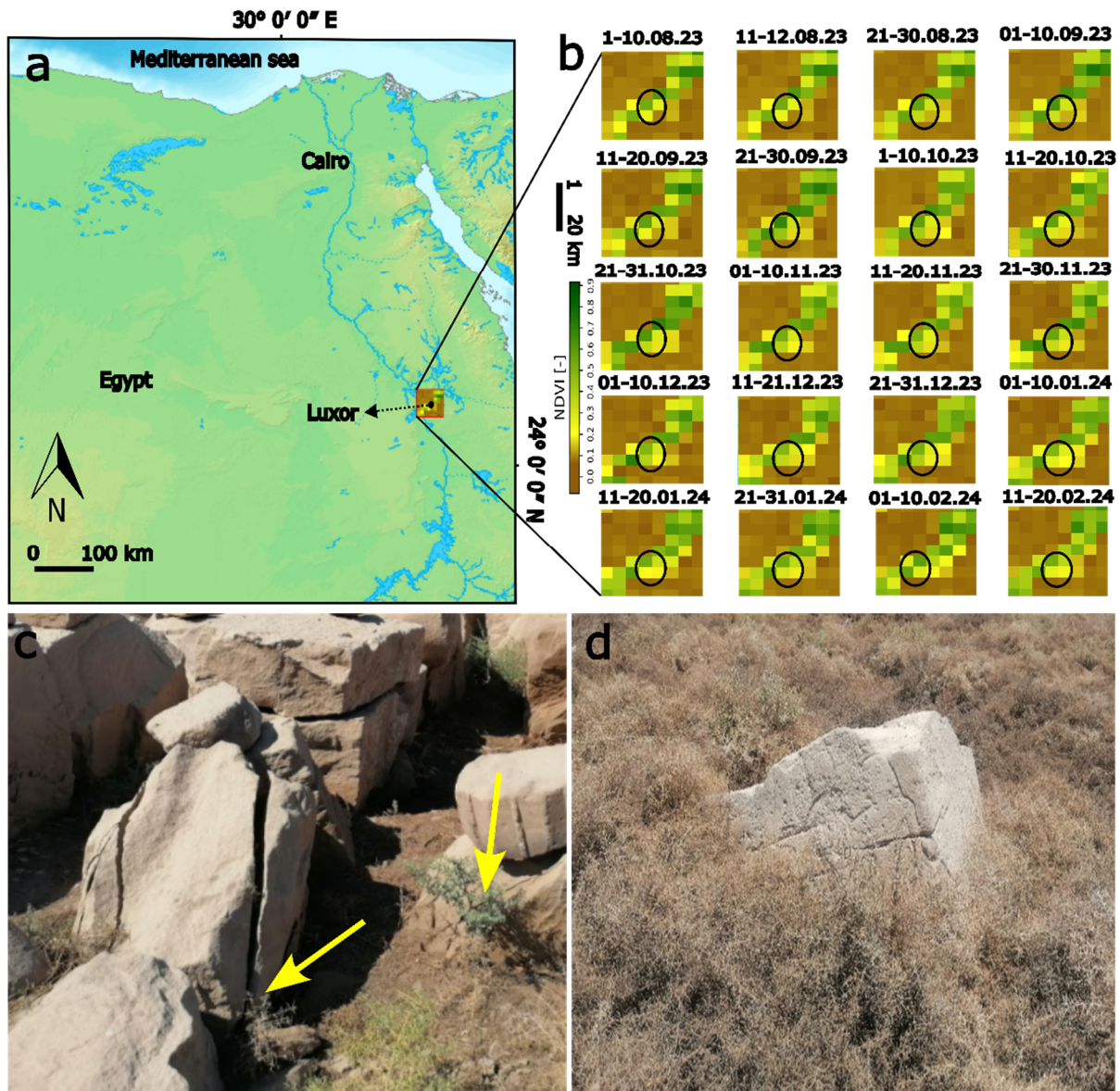


Figure 12. (a) General map of Egypt indicating the Luxor area with the NDVI Index. (b) Multi-temporal monitoring for the vegetation variations in Luxor and the case study area using the NDVI Index. (c,d) Loss of mechanical strength and physical and aesthetic properties due to the biodeterioration of the stone blocks and shown by yellow arrows.

Table 4. Temporal variation of vegetation coverage and density in Luxor city, particularly in the Karnak area, based on the NDVI values.

Month/Period	NDVI Range (Coverage)	Vegetation Coverage	NDVI Range (Density)	Vegetation Density
August 2023 (early)	Near 0 to 0.1	Bare soil/sparse vegetation	0.1–0.5	Sparse vegetation
August 2023 (late)	0.1–0.5	Sparse vegetation	0.5–0.6	Moderately dense vegetation
September 2023	0.1–0.5	Sparse vegetation	0.5–0.6	Increasingly dense vegetation
January 2024 (late)	Near 0 to 0.2	Bare soil/sparse vegetation	0.1–0.3	Sparse vegetation
February 2024 (early)	0.5–0.7	Dense vegetation	0.6 and up	Dense green vegetation

Plants with spinous structures, such as *Atraphaxis* and thorns/spines/prickles, were found to be superior plants that cause biodegradation to the stone blocks. The physical and morphological features of the plants indicated their impact on the mechanical damage of the stone and caused separation and fracturing of stone blocks (Figure 12c). In this regard, the biodeterioration on stones can be classified into physical/mechanical, chemical, and aesthetic [77]. Mechanically, the growth and movements of plants and organisms cause irreversible deformations under permanent loads. Chemically, some organisms and plants use the internal components of the stones as food materials (assimilation). In addition, plants and organisms can produce substances (dissimilatory), such as acids, that lead to chemical alteration and etching to the stone surfaces. Furthermore, plants and organisms can affect the aesthetical characteristics of stone due to the metabolism and byproducts causing encrustation and biofilms.

9. Restoration and Conservation Plan for Sandstone Blocks at Karnak

The sandstone blocks at Karnak have been subjected to various environmental factors, such as temperature fluctuations, wind erosion, salt weathering, contaminated water infiltration, and mechanical loads. To effectively conserve and restore the blocks, a comprehensive plan is required, with a focus on constructing new mastabas (elevated platforms) to prevent soil and water contact and to create an open museum setting for the Karnak site. Accordingly, for suitable restoration and conservation strategy, the next steps can be implemented, such as (1) constructing the mastabas (Elevated Platforms); (2) addressing decay mechanisms; (3) water management and contamination prevention; (4) conservation of affected blocks; (5) establishing an open museum; and (6) long-term preservation strategies.

The primary aim is to lift the sandstone blocks off the ground, minimizing direct contact with soil and water sources, thus preventing further water-related degradation, such as salt weathering and clay swelling. The mastabas (Figure 13a–d) should be constructed from durable, non-porous materials, like granite. In addition, each platform should be raised high enough to prevent capillary action from drawing contaminated water into the blocks, around 40–60 cm (Figure 13b). Drainage systems can be integrated around the mastabas to direct water away from the blocks. Survey and assess the condition of each sandstone block to determine specific restoration needs before relocation and use appropriate lifting and handling techniques to avoid further structural damage during the process of raising the blocks onto the mastabas. A protective layer (e.g., waterproof membranes) can be applied between the block and the platform to ensure complete isolation from moisture and water infiltration. Additionally, implement air circulation systems to avoid moisture buildup under the blocks and future decay. For restoration of the blocks heavily affected by surface erosion or salt weathering, mechanical and chemical cleaning methods should be employed carefully to restore the blocks. Using non-invasive cleaning techniques, such as micro-sandblasting or laser cleaning, for removing salt crusts, stains, and surface contaminants is considered a good option in case of their availability. Furthermore, consolidation treatments using ethyl silicate-based or lime-based solutions strengthen weak or fragmented stone areas and prevent further disintegration. In areas where the stone blocks have suffered structural damage, careful repair using compatible materials should be undertaken. Cracks can be filled with lime mortar.

For management and sustainable development, the relocated and restored sandstone blocks can be displayed as part of an open museum in the Karnak Temples. Each block should have informational signage detailing its original location, historical significance, and the restoration process it underwent. Moreover, designated pathways for visitors should be constructed to ensure easy access while minimizing direct human interaction with the blocks. These paths should be made from non-invasive materials that will not contribute to further contamination. Regular monitoring of the blocks' condition should be carried out using techniques like 3D scanning to track any signs of decay or deterioration.

Finally, a preventive conservation schedule should be established for cleaning, desalination, and reapplying protective coatings as necessary.

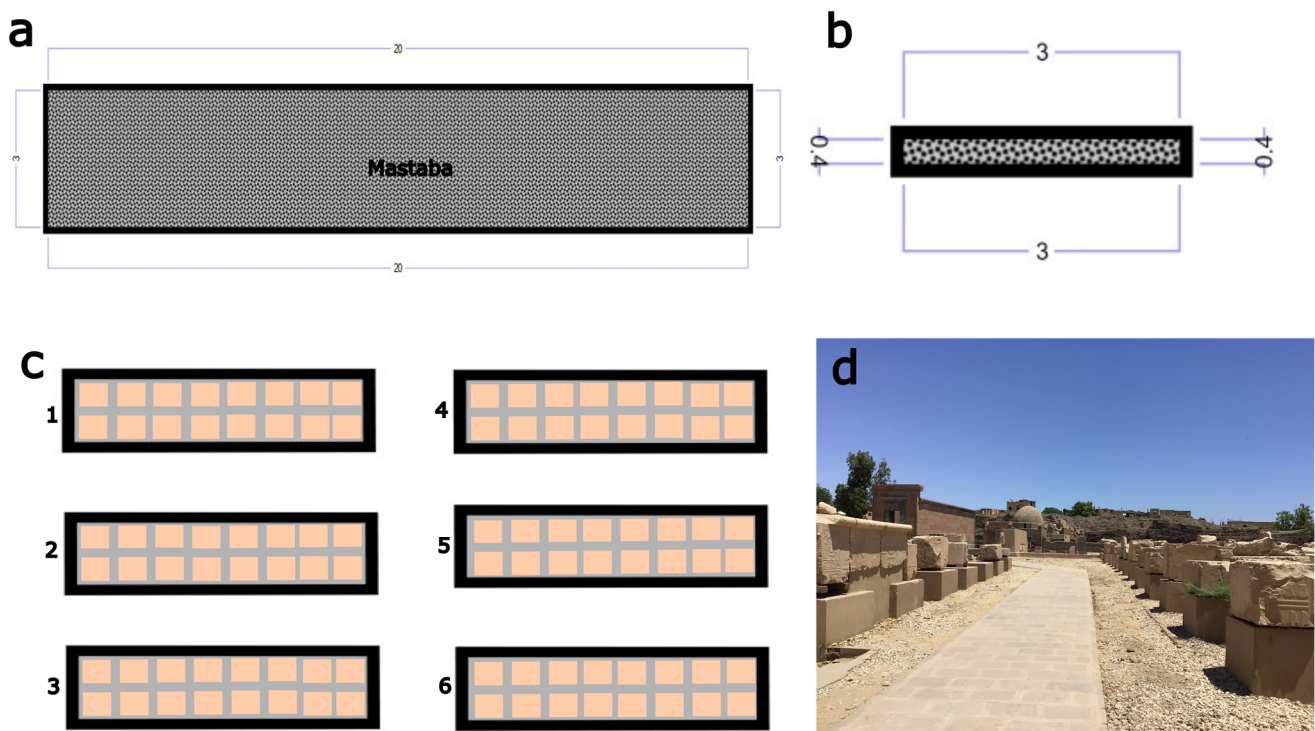


Figure 13. (a) The dimension of a Mastaba (20 m × 3 m); (b) cross-section of a Mastaba and its dimensions (3 m × 40 cm); (c) suggested system for six Mastabas constructions to lift around 144 stone blocks in the northeast corner (phase 1) over them. (d) Conducted a previous project to lift the stone blocks upon the Mastabas as part of the Karnak Open Museum (in front of the chapel of Hatshepsut), executed by the Egyptian Ministry of Tourism and Antiquity.

10. Conclusions

This detailed study of the stone blocks in the northeast corner of the Karnak Temples has exposed a range of sustainability challenges attributed to various mechanical and geochemical damage factors. In situ assessments reveal that these stone blocks are suffering from substantial structural degradation, including dismantling fractures and scattering. This damage is primarily the result of seismic activities, flooding events, and anthropogenic interference. The assessment also underscores the detrimental effects of contaminated water sources, adverse climatic conditions, and invasive vegetation on the durability of the stone. Multi-temporal satellite imagery has proven invaluable in tracking changes in vegetation coverage, which, in turn, influences the degradation process. These findings highlight the urgent need for ongoing monitoring, comprehensive documentation, and the application of advanced conservation techniques to ensure the preservation of the Karnak Temples.

Looking forward, future research should focus on several key areas to enhance the understanding and management of these challenges. This includes the application of non-destructive testing (NDT) methods to assess the condition of the materials without causing further damage. Detailed classification and analysis of the materials will be crucial for developing tailored conservation strategies. Additionally, the formulation of extensive restoration and site management strategies is essential for addressing the multi-faceted issues identified. Such strategies should incorporate robust conservation methods designed to protect the historical and cultural significance of the Karnak Temples for future generations. Interdisciplinary collaboration will be critical in this endeavor, integrating

expertise from archaeology, geology, and conservation to tackle the complex challenges associated with preserving this ancient heritage site.

To effectively manage and mitigate the identified challenges, a comprehensive conservation and restoration strategy must be implemented. Key components of this strategy include the construction of elevated platforms to reduce soil and water contact with the stone blocks. These platforms should be designed from durable materials, like granite, and raised sufficiently (40–60 cm) to prevent capillary action and water infiltration. Integrated drainage systems around these platforms will help direct water away from the blocks, further protecting them from moisture-related damage.

Addressing the decay mechanisms involves employing non-invasive cleaning techniques, such as micro-sandblasting or laser cleaning, to remove salt crusts and surface contaminants. Consolidation treatments using ethyl silicate-based or lime-based solutions will strengthen weakened areas of the stone. Effective water management and contamination prevention measures are also crucial. Protective layers, such as waterproof membranes, should be applied between the blocks and platforms to prevent moisture infiltration and air circulation systems can mitigate moisture buildup under the blocks.

For blocks suffering from severe erosion or salt weathering, careful restoration using compatible materials is necessary. Cracks should be filled with lime mortar and structural repairs should be conducted with a focus on maintaining historical accuracy. The creation of an open museum setting to display the relocated and restored blocks will enhance public understanding and appreciation of the site. Informational signage detailing the blocks' original locations, historical significance, and restoration processes will further educate visitors.

Long-term preservation efforts should include regular monitoring using advanced techniques, such as 3D scanning, to track the condition of the blocks and detect early signs of deterioration. A preventive conservation schedule should be established, incorporating periodic cleaning, desalination, and reapplication of protective coatings to ensure ongoing protection of the stone blocks.

Author Contributions: Conceptualization, A.F., E.M.-P. and S.D.-B.; writing—original draft preparation, A.F.; writing—review and editing, A.F.; visualization, A.F.; supervision, E.M.-P. and S.D.-B. All authors have read and agreed to the published version of the manuscript.

Funding: This research received no external funding.

Data Availability Statement: Data sharing is not applicable to this article, as no datasets were generated or analysed during the current study.

Conflicts of Interest: The authors declare no conflict of interest.

References

1. Wang, F.; Frühwirt, T.; Konietzky, H. Influence of repeated heating on physical-mechanical properties and damage evolution of granite. *Int. J. Rock Mech. Min. Sci.* **2020**, *136*, 104514. [CrossRef]
2. Brimblecombe, P. Environment and architectural stone. In *Springer eBooks*; Springer: Berlin/Heidelberg, Germany, 2014; pp. 317–347. [CrossRef]
3. Brimblecombe, P. Heritage Climatology. In *Climate Change and Cultural Heritage: Proceedings of the Ravello International Workshop, 14–16 May 2009 and Strasbourg European Master-Doctorate Course, 7–11 September 2009*; Edipuglia: Bari, Italy, 2010; pp. 54–57. Available online: https://www.getty.edu/conservation/publications_resources/teaching/pdf/stone_conservation/module4/7_SO.Brimblecombe.14May13a.pdf (accessed on 7 July 2024).
4. Ito, W.H.; Scussiato, T.; Vagnon, F.; Ferrero, A.M.; Migliazza, M.R.; Ramis, J.; De Queiroz, P.I.B. On the Thermal Stresses due to Weathering in Natural Stones. *Appl. Sci.* **2021**, *11*, 1188. [CrossRef]
5. Founda, D.; Katavoutas, G.; Pierros, F.; Mihalopoulos, N. Centennial changes in heat waves characteristics in Athens (Greece) from multiple definitions based on climatic and bioclimatic indices. *Glob. Planet. Change* **2022**, *212*, 103807. [CrossRef]
6. Livada, I.; Santamouris, M.; Niachou, K.; Papanikolaou, N.; Mihalakakou, G. Determination of places in the great Athens area where the heat island effect is observed. *Theor. Appl. Climatol.* **2002**, *71*, 219–230. [CrossRef]
7. Katavoutas, G.; Founda, D.; Kitsara, G.; Giannakopoulos, C. Climate change and thermal comfort in top tourist Destinations—The case of Santorini (Greece). *Sustainability* **2021**, *13*, 9107. [CrossRef]

8. Shi, X.J.; Shi, X.F. Numerical prediction on erosion damage caused by wind-blown sand movement. *Eur. J. Environ. Civ. Eng.* **2014**, *18*, 550–566. [CrossRef]
9. Belfiore, C.; Calabrò, C.; Ruffolo, S.; Ricca, M.; Török, Á.; Pezzino, A.; La Russa, M. The susceptibility to degradation of stone materials used in the built heritage of the Ortygia island (Syracuse, Italy): A laboratory study. *Int. J. Rock Mech. Min. Sci.* **2021**, *146*, 104877. [CrossRef]
10. Striani, R.; Cappai, M.; Casnedi, L.; Corcione, C.E.; Pia, G. Coating's influence on wind erosion of porous stones used in the Cultural Heritage of Southern Italy: Surface characterisation and resistance. *Case Stud. Constr. Mater.* **2022**, *17*, e01501. [CrossRef]
11. Fahmy, A.; Domínguez-Bella, S.; Martínez-López, J.; Molina-Piernas, E. Sand dune movement and flooding risk analysis for the pyramids of Meroe, Al Bagrawiya archaeological site, Sudan. *Herit. Sci.* **2023**, *11*, 136. [CrossRef]
12. Hemeda, S.; Fahmy, A.; Sonbol, A. Geo-Environmental and structural problems of the first successful true pyramid, (Snefru Northern Pyramid) in Dahshur, Egypt. *Geotech. Geol. Eng.* **2018**, *37*, 2463–2484. [CrossRef]
13. The Getty Conservation Institute. Archaeological Sites: Conservation and management. In *Readings in Conservation*; Sullivan, S., Mackay, R., Eds.; Getty Conservation Institute: Los Angeles, CA, USA, 2012; Available online: <https://www.getty.edu/publications/resources/virtuallibrary/9781606061244.pdf> (accessed on 12 July 2024).
14. Reader, C.D. A Geomorphological Study of the Giza Necropolis, with Implications for the Development of the Site. *Archaeometry* **2001**, *43*, 149–165. [CrossRef]
15. Faranda, D.; Ginesta, M.; Alberti, T.; Coppola, E.; Anzidei, M. Attributing Venice Acqua Alta events to a changing climate and evaluating the efficacy of MoSE adaptation strategy. *Npj Clim. Atmos. Sci.* **2023**, *6*, 181. [CrossRef]
16. Carbognin, L.; Teatini, P.; Tomasin, A.; Tosi, L. Global change and relative sea level rise at Venice: What impact in term of flooding. *Clim. Dyn.* **2009**, *35*, 1039–1047. [CrossRef]
17. Oliveira, C.S. Seismic Vulnerability of Historical Constructions: A Contribution. *Bull. Earthq. Eng.* **2003**, *1*, 37–82. [CrossRef]
18. Kázmér, M. Damage to Ancient Buildings from Earthquakes. In *Springer eBooks*; Springer: Berlin/Heidelberg, Germany, 2015; pp. 500–506. [CrossRef]
19. Park, H.; Ha, J.; Kim, S.; Jo, S. Seismic performance of ancient masonry structures in Korea rediscovered in 2016 M 5.8 Gyeongju earthquake. *Sustainability* **2019**, *11*, 1565. [CrossRef]
20. Marco, S. Recognition of earthquake-related damage in archaeological sites: Examples from the Dead Sea fault zone. *Tectonophysics* **2008**, *453*, 148–156. [CrossRef]
21. Sallam, M.A.; Hassan, H.M.; Sayed, M.A.; Hafiez HE, A.; Zahra, H.S.; Salem, M. Seismic vulnerability assessment of historical minarets in Cairo. *Geoenviron. Disasters* **2023**, *10*, 30. [CrossRef]
22. Bottari, C.; Capizzi, P.; Sortino, F. Unraveling the Seismic Source in Archaeoseismology: A combined approach on local site effects and geochemical data integration. *Heritage* **2024**, *7*, 427–447. [CrossRef]
23. Kreibich, H.; Thieken, A.H.; Grunenberg, H.; Ullrich, K.; Sommer, T. Extent, perception and mitigation of damage due to high groundwater levels in the city of Dresden, Germany. *Nat. Hazards Earth Syst. Sci.* **2009**, *9*, 1247–1258. [CrossRef]
24. Bork, M.; Lange, J.; Graf-Rosenfellner, M.; Hensen, B.; Olsson, O.; Hartung, T.; Fernández-Pascual, E.; Lang, F. Urban storm water infiltration systems are not reliable sinks for biocides: Evidence from column experiments. *Sci. Rep.* **2021**, *11*, 7242. [CrossRef]
25. Delgado, J.M.P.Q.; Guimarães, A.S.; De Freitas, V.P.; Antepara, I.; Kočí, V.; Černý, R. Salt damage and rising damp treatment in building structures. *Adv. Mater. Sci. Eng.* **2016**, *2016*, 1280894. [CrossRef]
26. Lasaponara, R.; Murgante, B.; Elfadaly, A.; Qelichi, M.; Shahraki, S.; Wafa, O.; Attia, W. Spatial Open Data for Monitoring Risks and Preserving Archaeological Areas and Landscape: Case Studies at Kom el Shoqafa, Egypt and Shush, Iran. *Sustainability* **2017**, *9*, 572. [CrossRef]
27. Fahmy, A.; Gołabiewska, A.; Wojnicz, W.; Stanisławska, A.; Kowalski, J.; Łuczak, J.; Zaleska-Medynska, A.; Domínguez-Bella, S.; Martínez-López, J.; Molina-Piernas, E. Multi-functional monodispersed SiO₂-TiO₂ core-shell nanostructure and TEOS in the consolidation of archaeological lime mortars surfaces. *J. Build. Eng.* **2023**, *79*, 107809. [CrossRef]
28. Fouad, S.S.; Heggy, E.; Weilacher, U. Waterways transformation in the vulnerable port city of Alexandria. *Cities* **2023**, *141*, 104426. [CrossRef]
29. Oguchi, C.T.; Yu, S. A review of theoretical salt weathering studies for stone heritage. *Prog. Earth Planet. Sci.* **2021**, *8*, 32. [CrossRef]
30. Lubelli, B.; Van Hees, R.P.; Groot, C.J. The role of sea salts in the occurrence of different damage mechanisms and decay patterns on brick masonry. *Constr. Build. Mater.* **2004**, *18*, 119–124. [CrossRef]
31. Rombolà, R.M. The GIS for Urban Analysis and Risk Map of Archaeological Site: The Case of Sphinxes Avenue in Luxor. In *Sustainable Conservation and Urban Regeneration. Research for Development*; Folli, M., Ed.; Springer: Cham, Switzerland, 2018. [CrossRef]
32. Fitzner, B.; Heinrichs, K.; la Bouchardiere, D. Weathering damage on Pharaonic sandstone monuments in Luxor-Egypt. *Build. Environ.* **2003**, *38*, 1089–1103. [CrossRef]
33. Ahmed, A.A. Land use change and deterioration of pharaonic monuments in upper Egypt. *J. Eng. Sci. Assiut Univ.* **2009**, *37*, 161. Available online: https://jesaun.journals.ekb.eg/article_121202_46d5400d2a495a6626e99b8e8331681d.pdf (accessed on 10 July 2024). [CrossRef]
34. Megahed, H.A. Hydrological and archaeological studies to detect the deterioration of Edfu temple in Upper Egypt due to environmental changes during the last five decades. *SN Appl. Sci.* **2020**, *2*, 1952. [CrossRef]

35. Marey Mahmoud, H.; Kantiranis, N.; Stratis, J. Salt damage on the wall paintings of the festival temple of Thutmose III, Karnak Temples Complex, Upper of Egypt. A case study. *Int. J. Commun. Syst.* **2010**, *1*, 133–142.
36. Fahmy, A.; Martínez-López, J.; Sánchez-Bellón, A.; Domínguez-Bella, S.; Molina-Piernas, E. Multianalytical diagnostic approaches for the assessment of materials and decay of the archaeological sandstone of Osiris Temple (The Abaton) in Bigeh Island, Philae (Aswan, Egypt). *J. Cult. Herit.* **2022**, *58*, 167–178. [CrossRef]
37. Fahmy, A.; Molina-Piernas, E.; Martínez-López, J.; Domínguez-Bella, S. Salt weathering impact on Nero/Ramses II Temple at El-Ashmonein archaeological site (Hermopolis Magna), Egypt. *Herit. Sci.* **2022**, *10*, 125. [CrossRef]
38. Wilkinson, R.H. *The Complete Temples of Ancient Egypt*; Thames & Hudson: London, UK, 2000. [CrossRef]
39. Dieter, A. *The Encyclopedia of Ancient Egyptian Architecture*; Tauris, I.B., Ed.; Princeton University Press: Princeton, NJ, USA, 2002. Available online: <https://archive.org/search.php?query=external-identifier:%22urn:oclc:record:1033591802%22> (accessed on 11 July 2024).
40. Elaine, S. Introduction. In *Digital Karnak, Los Angeles*; University of California Santa Cruz: Santa Cruz, CA, USA, 2008. Available online: <http://dlib.etc.ucla.edu/projects/Karnak> (accessed on 11 July 2024).
41. Blyth, E. *Karnak: Evolution of a Temple*; Routledge: London, UK, 2006; ISBN 0-415-40486-X. Available online: https://api.pageplace.de/preview/DT0400.9781134136681_A24932187/preview-9781134136681_A24932187.pdf (accessed on 15 July 2024).
42. Ghilardi, M.; Boraik, M. Reconstructing the holocene depositional environments in the western part of Ancient Karnak temples complex (Egypt): A geoarchaeological approach. *J. Archaeol. Sci.* **2011**, *38*, 3204–3216. [CrossRef]
43. Ahmed, A.A.; Fogg, G.E.; Gameh, M.A. Water use at Luxor, Egypt: Consumption analysis and future demand forecasting. *Environ. Earth Sci.* **2014**, *72*, 1041–1053. [CrossRef]
44. Elkhateeb, S.O.; Dosoky, W.; Mohamed, A. Geoelectric and mineralogical studies for foundation soil characterization in new Luxor city, Upper Egypt. *Arab. J. Geosci.* **2022**, *15*, 1220. [CrossRef]
45. Harrell, J.A.; Storemyr, P. Ancient Egyptian quarries—An illustrated overview. In *QuarryScapes: Ancient Stone Quarry Landscapes in the Eastern Mediterranean*; Abu-Jaber, N., Bloxam, E.G., Degryse, P., Heldal, T., Eds.; Geological Survey of Norway Special Publication: Fribourg, Switzerland, 2009; Volume 12, pp. 7–50. Available online: https://www.ngu.no/upload/Publikasjoner/Special%20publication/SP12_s7-50.pdf (accessed on 17 July 2024).
46. Fahmy, A.; Molina-Piernas, E.; Martínez-López, J.; Machev, P.; Domínguez-Bella, S. Coastal Environment Impact on the Construction Materials of Anfushi's Necropolis (Pharos's Island) in Alexandria, Egypt. *Minerals* **2022**, *12*, 1235. [CrossRef]
47. Fahmy, A.; Molina-Piernas, E.; Domínguez-Bella, S.; Martínez-López, J.; Helmi, F. Geoenvironmental investigation of Sahure's pyramid, Abusir archeological site, Giza, Egypt. *Herit. Sci.* **2022**, *10*, 61. [CrossRef]
48. Nilsson, M.; Ward, J. Gebel el-Silsila throughout the Ages: Part 7-Late Period to Grieco Roman Era. 2021. Available online: <https://lucris.lub.lu.se/ws/portalfiles/portal/113150354/AE124NilssonGebel7.pdf> (accessed on 18 July 2024).
49. Nilsson, M.; Ward, J. Gebel el-Silsila throughout the Ages: Part 1. 2019. Available online: <https://lucris.lub.lu.se/ws/portalfiles/portal/101678193/AE113WardGebel1asublished.pdf> (accessed on 18 July 2024).
50. Nilsson, M.; Almasy, A. Quarrying for Claudius, protected by Min: A small quarry at Gebel el-Silsila East. *Br. Mus. Stud. Anc. Egypt Sudan* **2015**, *22*, 87–110. Available online: https://web.archive.org/web/20180409222029id_/http://www.britishmuseum.org/pdf/Nilsson_FINAL.pdf (accessed on 13 July 2024).
51. Elwaseif, M.; Ismail, A.; Abdalla, M.; Abdel-Rahman, M.; Hafez, M.A. Geophysical and hydrological investigations at the west bank of Nile River (Luxor, Egypt). *Environ. Earth Sci.* **2012**, *67*, 911–921. [CrossRef]
52. Mokhtar, M. Monitoring of Groundwater and Ancient Structures in Luxor and Karnak Temples. 2007. Available online: <https://arce.org/> (accessed on 13 July 2024).
53. Ismail, A.; Anderson, N.L.; Rogers, J.D.; Society of Exploration Geophysicists. Hydrogeophysical investigation at Luxor, Southern Egypt. *J. Environ. Eng. Geophys.* **2005**, *10*, 35–49. [CrossRef]
54. SECAP. Sustainable Energy and Climate Action Plan. City of Luxor, Governorate of Luxor—Egypt. 2017. Available online: [https://www.climamed.eu/wp-content/uploads/files/Egypt-Governorate-of-Luxor-Sustainable-Energy-and-Climate-Action-Plan-\(SECAP\).pdf](https://www.climamed.eu/wp-content/uploads/files/Egypt-Governorate-of-Luxor-Sustainable-Energy-and-Climate-Action-Plan-(SECAP).pdf) (accessed on 19 July 2024).
55. Qadri, S.T.; Mirza, M.Q.; Raja, A.; Yaghmaei-Sabegh, S.; Hakimi, M.H.; Ali, S.H.; Khan, M.Y. Application of Probabilistic Seismic Hazard Assessment to Understand the Earthquake Hazard in Attock City, Pakistan: A Step towards Linking Hazards and Sustainability. *Sustainability* **2023**, *15*, 1023. [CrossRef]
56. Karakhanyan, A.; Armenia, Y.; Avagyan, A.; Sourouzian, H. Archaeoseismological studies at the temple of Amenhotep III, Luxor, Egypt. In *Ancient Earthquakes: Geological Society of America Special Paper*; Sin tubin, M., Stewart, I.S., Niemi, T.M., Altunel, E., Eds.; Geological Society of America: Boulder, CO, USA, 2010; p. 471. [CrossRef]
57. El-Sayed, A.; Wahlström, R.; Kulhánek, O. Seismic hazard of Egypt. *Nat. Hazards* **1994**, *10*, 247–259. Available online: https://gfzpublic.gfz-potsdam.de/rest/items/item_232445_1/component/file_232444/content (accessed on 19 July 2024). [CrossRef]
58. Toonen WH, J.; Graham, A.; Pennington, B.T.; Hunter, M.A.; Strutt, K.D.; Barker, D.S.; Masson-Berghoff, A.; Emery, V.L. Holocene fluvial history of the Nile's west bank at ancient Thebes, Luxor, Egypt, and its relation with cultural dynamics and basin-wide hydroclimatic variability. *Geoarchaeology* **2018**, *33*, 273–290. [CrossRef]
59. Russell, C. Karnak before the Spade Arrived. 2005. Available online: https://www.researchgate.net/publication/348133958_Karnak_Before_the_French_Arrived (accessed on 20 July 2024).

60. Toonen WH, J.; Graham, A.; Masson-Berghoff, A.; Peeters, J.; Winkels, T.G.; Pennington, B.T.; Hunter, M.A.; Strutt, K.D.; Barker, D.S.; Emery, V.L.; et al. Amenhotep III's Mansion of Millions of Years in Thebes (Luxor, Egypt): Submergence of high grounds by river floods and Nile sediments. *J. Archaeol. Sci. Rep.* **2019**, *25*, 195–205. [CrossRef]
61. McLane, J.; Raphael AJ Wüst Porter, B.; Rutherford, J. Flash-Flood Impacts and Protection Measures in the Valley of the Kings, Luxor, Egypt. *APT Bull. J. Preserv. Technol.* **2003**, *34*, 37–45. [CrossRef]
62. Baines, J. The inundation stela of Sebekhotpe VIII. *Acta Orient.* **1974**, *36*, 39–54. Available online: <https://ora.ouls.ox.ac.uk/objects/uuid:f0914ff3-bc93-4525-951d-870f1782fe99> (accessed on 20 July 2024).
63. Rodríguez-Pascua, M.A.; Pérez-López, R.; Giner-Robles, J.L.; Garduño-Monroy, V.H. A comprehensive classification of Earthquake Archaeological Effects (EAE) in archaeoseismology: Application to ancient remains of Roman and Mesoamerican cultures. *Quat. Int.* **2011**, *242*, 20–30. [CrossRef]
64. Yön, B.; Sayin, E.; Onat, O. Earthquakes and structural damages. In *InTech eBooks*; IntechOpen: London, UK, 2017. [CrossRef]
65. Feilden, B.; Alva, A. Earthquakes and Historic Buildings. 1993. Available online: <https://openarchive.icomos.org/id/eprint/843/1/ro29.pdf> (accessed on 22 July 2024).
66. Hughes, R. The effects of flooding upon the buildings in developing countries. *Disasters* **1982**, *6*, 183–194. Available online: <https://www.eird.org/bibliovirtual/riesgo-urbano/pdf/eng/doc12030/doc12030-a.pdf> (accessed on 22 July 2024). [CrossRef]
67. Wilk, K. Hazards for buildings and structures caused by flood conditions. *E3S Web Conf.* **2018**, *45*, 00101. [CrossRef]
68. Shen, Y.-J.; Zhang, Y.-L.; Gao, F.; Yang, G.-S.; Lai, X.-P. Influence of Temperature on the Microstructure Deterioration of Sandstone. *Energies* **2018**, *11*, 1753. [CrossRef]
69. Kompaníková, Z.; Gomez-Heras, M.; Michňová, J.; Durmeková, T.; Vlčko, J. Sandstone alterations triggered by fire-related temperatures. *Environ. Earth Sci.* **2014**, *72*, 2569–2581. [CrossRef]
70. Liang, Z.; Wu, Z.; Yao, W.; Noori, M.; Yang, C.; Xiao, P.; Leng, Y.; Deng, L. Pisha sandstone: Causes, processes and erosion options for its control and prospects. *Int. Soil Water Conserv. Res.* **2019**, *7*, 1–8. [CrossRef]
71. Richards, J.; Viles, H.; Guo, Q. The importance of wind as a driver of earthen heritage deterioration in dryland environments. *Geomorphology* **2020**, *369*, 107363. [CrossRef]
72. Alves, C.; Figueiredo, C.A.M.; Sanjurjo-Sánchez, J.; Hernández, A.C. Salt Weathering of Natural Stone: A Review of Comparative Laboratory Studies. *Heritage* **2021**, *4*, 1554–1565. [CrossRef]
73. Zehnder, K.; Arnold, A. Crystal growth in salt efflorescence. *J. Cryst. Growth* **1989**, *97*, 513–521. [CrossRef]
74. Cardell, C.; Delalieux, F.; Roumpopoulos, K.; Moropoulou, A.; Auger, F.; van Grieken, R. Salt-induced decay in calcareous stone monuments and buildings in a marine environment in SW France. In *Construction and Building Materials*; Elsevier Ltd.: Amsterdam, The Netherlands, 2003; Volume 17. [CrossRef]
75. De Oliveira, R.; Guallichico, L.A.G.; Policarpo, E.; Cadore, A.R.; Freitas, R.O.; da Silva, F.M.C.; de CTeixeira, V.; Paniago, R.M.; Chacham, H.; Matos, M.J.S.; et al. High throughput investigation of an emergent and naturally abundant 2D material: Clinocllore. *Appl. Surf. Sci.* **2022**, *599*, 153959. [CrossRef]
76. Elert, K.; Rodríguez-Navarro, C. Degradation and conservation of clay-containing stone: A review. In *Construction and Building Materials*; Elsevier Ltd.: Amsterdam, The Netherlands, 2022; Volume 330. [CrossRef]
77. Cozzolino, A.; Adamo, P.; Bonanomi, G.; Motti, R. The Role of Lichens, Mosses, and Vascular Plants in the Biodeterioration of Historic Buildings: A Review. *Plants* **2022**, *11*, 3429. [CrossRef]

Disclaimer/Publisher's Note: The statements, opinions and data contained in all publications are solely those of the individual author(s) and contributor(s) and not of MDPI and/or the editor(s). MDPI and/or the editor(s) disclaim responsibility for any injury to people or property resulting from any ideas, methods, instructions or products referred to in the content.